Review Article

Preclinical and clinical studies of anticancer agent-incorporating polymer micelles

Yasuhiro Matsumura[1,3] and Kazunori Kataoka[2]

[1]Investigative Treatment Division, Research Center for Innovative Oncology, National Cancer Center Hospital East, 6-5-1 Kashiwanoha, Kashiwa 277-8577; [2]Department of Materials Engineering, Graduate School of Engineering, The University of Tokyo, 7-3-1 Hongo, Bunkyo-ku, Tokyo 113-8656, Japan

(Received November 17, 2008/Revised December 25, 2008/Accepted December 25, 2008/Online publication February 17, 2009)

The size of anticancer agent-incorporating micelles can be controlled within the diameter range of 20–100 nm to ensure that they do not penetrate normal vessel walls. With this development, it is expected that the incidence of drug-induced side-effects may be decreased owing to the reduced drug distribution in normal tissue. Micelle systems can also evade non-specific capture by the reticuloendothelial system because the outer shell of a micelle is covered with polyethylene glycol. Consequently, a polymer micelle carrier can be delivered selectively to a tumor by utilizing the enhanced permeability and retention effect. Moreover, a water-insoluble drug can be incorporated into polymer micelles. Presently, several anticancer agent-incorporating micelle carrier systems are under preclinical and clinical evaluation. Furthermore, nucleic acid-incorporating micelle carrier systems are also being developed. (*Cancer Sci* 2009; 100: 572–579)

Nanotechnology is one of the fast-moving technologies and is presently contributing significantly to the progress of medical science. Drugs categorized under the drug delivery system (DDS) are made primarily by utilizing nanotechnology. In the field of oncology, DDS drugs have been produced and evaluated in preclinical or clinical trials, with some already approved for clinical use (Table 1). More specifically, DDS can be used for active or passive targeting of tumor tissues. Passive targeting refers to the development of monoclonal antibodies directed against tumor-related molecules, allowing targeting of a tumor from the specific binding of antibodies with respective antigens. However, the application of DDS using monoclonal antibodies is restricted to tumors expressing high levels of related antigens.

Passive targeting can be achieved by utilizing the enhanced permeability and retention (EPR) effect.[1,2] This effect is based on the pathophysiological characteristics of solid tumor tissues, namely, hypervascularity, incomplete vascular architecture, secretion of vascular permeability factors stimulating extravasation within cancer tissue, and absence of effective lymphatic drainage from tumors that impedes the efficient clearance of macromolecules accumulated in solid tumor tissues (Fig. 1A,B).

Several techniques have been developed to maximally utilize the EPR effect such as modification of drug structures and development of drug carriers. Polymeric micelle-based anticancer drugs were originally developed by Kataoka *et al.* in the late 1980s or early 1990s.[3–5] Polymeric micelles were expected to increase the accumulation of drugs in tumor tissues by utilizing the EPR effect as well as to incorporate various kinds of drugs into their inner core with relatively high stability by chemical conjugation or physical entrapment. Also, the size of micelles can be controlled within the diameter range of 20–100 nm to ensure that they do not penetrate normal vessel walls. With this development, it is expected that the incidence of drug-induced side-effects may be decreased owing to the reduced drug distribution in normal tissues.

Table 1. Examples of drug delivery systems in oncology and their stage of development

Passive targeting

Name	Platform	Compound	Clinical stage
NK105	Micelles	Paclitaxel	P2
NC-6004	Micelles	Cisplatin	P1/2
NK012	Micelles	SN-38	P2
Smancs	Polymer conjugate	Neocarzinostatin	Approved
Doxil	Liposome	Doxorubicin	Approved
Abraxane	Albumin particle	Paclitaxel	Approved
Xyotax	Polymer conjugate	Paclitaxel	P3
CT-2106	Polymer conjugate	Camptothecin	P2
EndoTAG	Cationic Liposome	Paclitaxel	P2
MAG-CPT	Polymer conjugate	Camptothecin	P1
LE-SN-38	Liposome	SN-38	P2
PK1	Polymer conjugate	Doxorubicin	P2
,hT-101	Polymer conjugate	Camptothecin	P2
SP1049C	Micelles	Doxorubicin	P3
CPX-1	Liposome	CPT-11,floxuridine	P2

Active targeting

Name	Platform	Compound	Clinical Stage
Mylotarg	Anti-CD33-Ab	Calicheamicin	Approved
Zevalin	Anti-CD20-Ab	90Y	Approved
Bexxar	Anti-CD20-Ab	131 I	Approved
PK2	Galactose-Polymer	Doxorubicin	P1
MCC465	Ab-liposome	Doxorubicin	P1
MBP-426	Transferrin-liposome	Oxaliplatin	P1
CALAA-01	Transferrin-polymer	siRNA	P1
T-DM1	Anti-HER2-Ab	DM1	P1

In this paper, we review recent developments in polymeric micelle systems presently being evaluated in clinical trials and introduce new micellar formulations.

Anticancer agent-incorporating micelle carrier systems under clinical evaluation

NK105: paclitaxel (PTX)-incorporating micellar nanoparticle

Background. PTX is one of the most useful anticancer agents against various cancers, including ovarian, breast and lung cancers.[6,7] However, it produces serious adverse effects such as neutropenia and peripheral sensory neuropathy. In addition, anaphylaxis and other severe hypersensitive reactions have been reported in 2–4% of patients receiving the drug even after

[3]To whom correspondence should be addressed. E-mail: yhmatsum@east.ncc.go.jp

doi: 10.1111/j.1349-7006.2009.01103.x

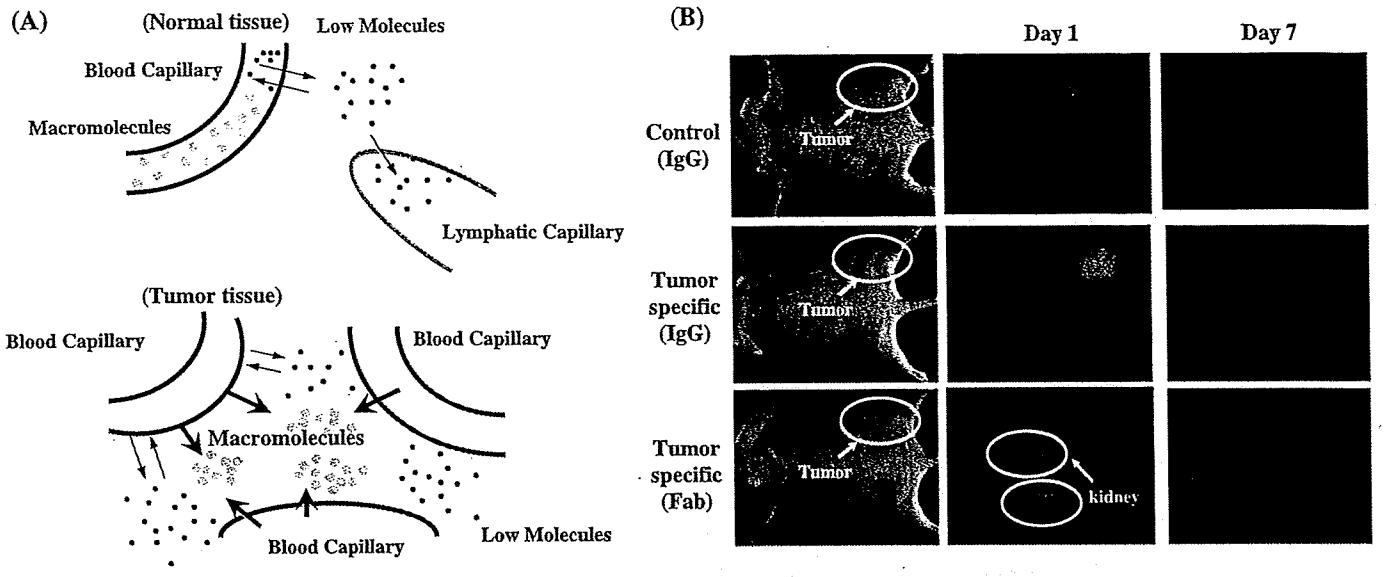

Fig. 1. (A) A diagram of normal and tumor tissue, demonstrating the presence of a lymphatic duct in normal tissue (upper) but the absence of any lymphatic duct in tumor tissue (lower). Small molecules easily leak from normal vessels in the body, which gives small molecules a short plasma half life. On the other hand, macromolecules have a long plasma half life because they are too large to pass through the normal vessel walls, unless they are trapped by the reticuloendothelial system in various organs. In the solid tumor tissues shown in the lower panel, it was found that solid tumors generally possess several pathophysiological characteristics: hypervasculature, secretion of vascular permeability factors stimulating extravasation of macromolecules within the cancer, and absence of effective lymphatic drainage from tumors that impedes the efficient clearance of macromolecules accumulated in solid tumor tissues. These characteristics of solid tumors are the basis of the enhanced permeability and retention (EPR) effect. Summarizing these findings, conventional low-molecular-weight anticancer agents disappear before reaching the tumor tissues and exerting their cell-killing effect. On the other hand, macromolecules and nanoparticles including micelle carriers should have time to reach the tumor, extravasate from the tumor capillaries, and stay for a long time in the tumor tissue, by means of the EPR effect. (B) Example of the EPR effect. This *in vivo* imaging demonstrates that both control whole immunoglobulin G (IgG) and the specific whole monoclonal antibody (mAb) accumulated selectively in the tumor tissue on day 1 after invravenous injection. On day 7, a greater degree of retention of the specific whole mAb as compared to the control IgG was noted. On the other hand, the F(ab) region of the specific mAb with a molecular weight of 45 000 accumulated in the tumor to the same extent as the control whole IgG. Interestingly, fluorescence of the F(ab) could also be detected in both the kidneys, which implied that the antigen binding fragment F(ab) could easily pass through the kidney glomerulus. This accumulation of the control IgG in the tumor represents the EPR effect. The findings suggest that not only the specific affinity of the mAb, but also the size of the molecules and the stability of the molecules in blood are important for tumor-selective targeting.

premedication with anti-allergic agents; these adverse reactions have been attributed to the mixture of Cremophor EL and ethanol used for solubilizing PTX.[8,9] Of the adverse reactions, neutropenia can be prevented or managed effectively by administering a granulocyte colony-stimulating factor. On the other hand, there are no effective therapies to prevent or reduce nerve damage associated with PTX-induced peripheral neuropathy. Thus, neurotoxicity constitutes a significant dose-limiting toxicity of the drug.[10,11]

Preparation and characterization of NK105. To construct NK105 micellar nanoparticles (Fig. 2A), block copolymers consisting of polyethylene glycol (PEG) and polyaspartate,[3–5] were used. PTX was incorporated into polymeric micelles formed by physical entrapment utilizing hydrophobic interactions between PTX and the block copolymer polyaspartate chain. NK105 was prepared by facilitating the self association of NK105 polymers and PTX. NK105 was obtained as a freeze-dried formulation and contained about 23% (w/w) of PTX The weight-average diameter of the nanoparticles was approximately 85 nm with a narrow size distribution.[12]

Preclinical studies. In an *in vivo* pharmacokinetics study using colon 26 tumor-bearing CDF1 mice, the plasma concentration at 5 min (C_{5min}) and the area under the curve (AUC) of NK105 were 11- to 20-fold and 50- to 86-fold higher than those of PTX. The maximum contentration (C_{max}) and AUC of NK105 in colon 26 tumors were approximately 3 and 25 times higher than those of PTX. NK105 continued to accumulate in the tumors until 72 h postinjection (data not shown).

In BALB/c mice bearing subcutaneous HT-29 colon cancer tumors, NK105 exhibited superior antitumor activity compared with PTX ($P < 0.001$). Tumor suppression by NK105 increased in a dose-dependent manner (Fig. 2B).

Paclitaxel treatment has been shown to cause cumulative sensory-dominant peripheral neurotoxicity in humans characterized clinically by numbness and/or paraesthesia of the extremities. Pathologically, axonal swelling, vesicular degeneration, and demyelination have also been observed. We therefore examined the pathologic effects of free PTX and NK105 using both electrophysiological and morphological methods. After drug administration for 2 months, the amplitude of the caudal sensory nerve action potential in the control group increased in association with rat maturation. The amplitude was significantly smaller in the PTX group than in the control group ($P < 0.01$); it was significantly larger in the NK105 group than in the PTX group ($P < 0.05$); and it was comparable between the NK105 group and the control group (Fig. 2C).

Clinical study. A phase I study was designed to determine the maximum tolerated dose (MTD), dose-limiting toxicities (DLTs), and recommended dose (RD) of NK105 for phase II, as well as its pharmacokinetics.[13]

NK105 was administered by intravenous infusion for 1 h every 3 weeks without anti-allergic premedication. The starting dose was 10 mg PTX equivalent/m^2, and the dose escalated according to the accelerated titration method. DLTs were observed in two patients at 180 mg/m^2 (grade 4 neutropenia lasting for more than 5 days), which was determined as MTD. Allergic reactions were not observed in any of the patients except in one. The RD was 150 mg/m^2. A partial response was observed in one pancreatic cancer patient who received more than 12 courses of NK105 (Fig. 2D). Colon and gastric cancer patients experienced

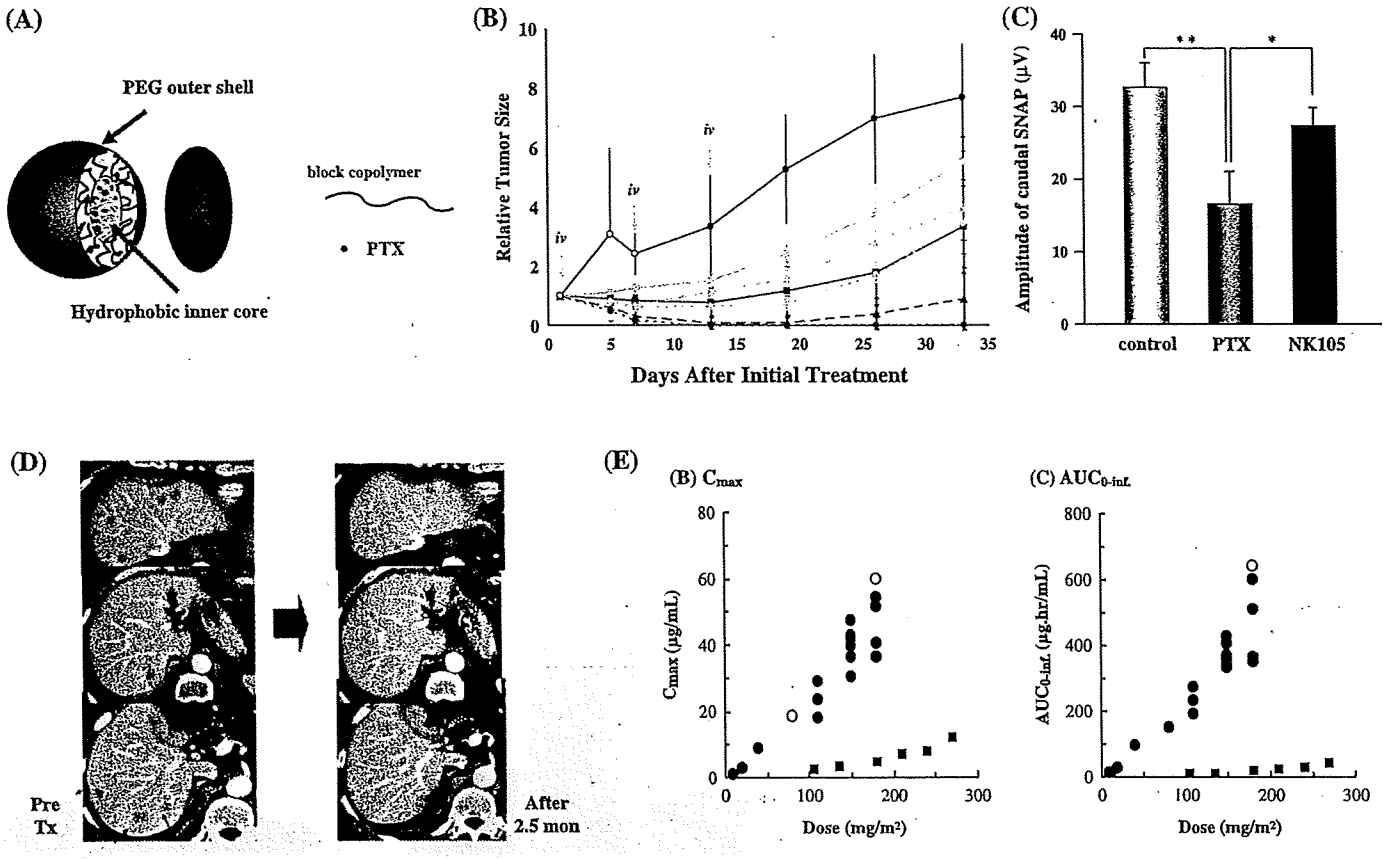

Fig. 2. (A) The schematic structure of NK105, a micelle-forming polymeric drug, that is a polyethylene glycol (PEG)-poly (aspartic acid) block copolymer conjugated with *paclitaxel* (PTX). NK105 was obtained as a freeze-dried formulation and contained approximately 23% (w/w) of PTX. The weight-average diameter of the nanoparticles was approximately 85 nm with a narrow size distribution. (B) Antitumor activity of PTX or NK105 on HT-29 human colon cancer xenografts.Each drug was administered intravenously weekly for 3 times at a PTX equivalent dose of 25 mg/kg, 50 mg/kg, or 100 mg/kg. Light blue lines show the treatment with PTX. Red lines show the treatment with NK105. NK105 exhibited significant superior antitumor activity as compared with PTX at respective dose levels ($P < 0.001$). Especially, tumors disappeared after the first dosing to mice treated with NK105 at 100 mg/kg. Dark blue line (control). Each point: mean ± SE. (C) The amplitude of caudal sensory nerve action potential after the drugs administration for 2 months. The amplitude was significantly smaller in the PTX group as compared to control or NK105 administration group. (D) Serial computed tomography scans. A 60-year-old man with pancreatic cancer who was treated with NK105 at a dose level of 150 mg/m². Baseline scan (left) showing multiple metastasis in the liver. Partial response, characterized by a more than 90% decrease in the size of the liver metastasis (right) compared with the baseline scan. The antitumor response was maintained for nearly 1 year. (E) Correlations between dosage and maximum contentration (C_{max}) and area under the curve (AUC) for both PTX (■) d NK105 (●). Both C_{max} and AUC of NK105 were significantly higher than those of PTX. Different from PTX, the Cmax and AUC of NK105 increased linearly at doses between 10 and 15 mg/m². The AUC of NK105 at the recommended dose was 10–30-fold higher than that of PTX at a conventional dose, 210 mg/m².

stable disease lasting for ten and seven courses, respectively. Despite long-term administration, only grade 1 or 2 neuropathy was observed when the dose or period of drug administration was modified. The C_{max} and AUC of NK105 showed dose-dependent characteristics. The plasma AUC of NK105 at 150 mg/m² was approximately 30-fold higher than that of the commonly used PTX formulation (Fig. 2E).

Dose-limiting toxicity was Grade 4 neutropenia. NK105 facilitates prolonged systemic PTX exposure in plasma. Tri-weekly 1-h infusion of NK105 was feasible and well tolerated, with antitumor activity. A phase II study of NK105 against advanced stomach cancer as a second-line therapy is currently underway.

NC-6004: cisplatin-incorporating micellar nanoparticle

Background. Cisplatin (*cis*-dichlorodiammineplatinum [II]: CDDP] is a key drug in the chemotherapy of various cancers, including lung, gastrointestinal and genitourinary cancers.[14,15] However, it is often necessary to discontinue CDDP treatment because of its adverse reactions (e.g. nephrotoxicity and neurotoxicity) despite its persisting effects.[16] To date, platinum analogs (e.g. carboplatin and oxaliplatin)[17] have been developed to overcome these CDDP-related disadvantages. Consequently, these analogs have become the standard drugs for ovarian[18] and colon[19] cancers. On the other hand, these regimens including CDDP constitute the standard treatment for lung, gastric, testicular[20] and urothelial[21] cancers. Therefore, the development of DDS technology is anticipated, which would enable better selective CDDP accumulation in solid tumors while lessening its distribution in normal tissue.

Preparation and characterization of NC-6004. NC-6004 was prepared according to a slightly modified procedure reported by Nishiyama *et al.*[22] (Fig. 3A). NC-6004 consists of PEG, a hydrophilic chain constituting the outer shell of micelles, and the coordinate complex of poly(glutamic acid) and CDDP, a polymer-metal complex-forming chain constituting the inner core of micelles. A narrowly distributed size of polymeric micelles (20 nm) was confirmed by dynamic light-scattering measurement. Also, static light-scattering measurement revealed that the CDDP-loaded micelles showed no dissociation upon dilution and the critical micellar concentration was $<5 \times 10^{-7}$,

doi: 10.1111/j.1349-7006.2009.01103.x

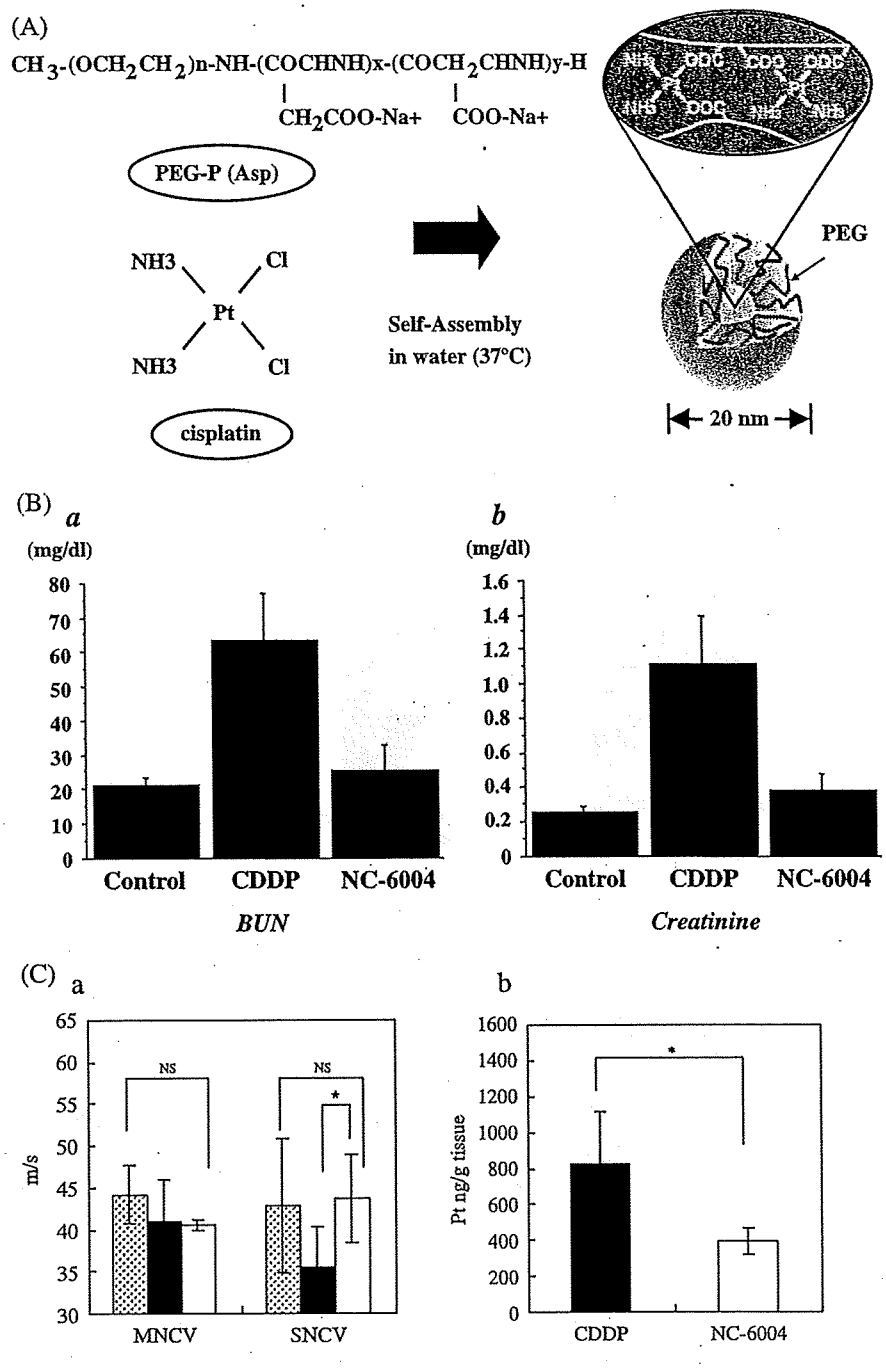

Fig. 3. (A) Cisplatin-incorporating polymeric micelles (NC-6004) consists of polyethylene glycol (PEG), a hydrophilic chain which constitutes the outer shell of the micelles, and the coordinate complex of Poly(Glu) and *cis*-dichlorodiammineplatinum (II) (CDDP) constitutes the inner core of the micelles. The mean particle size of NC-6004 was approximately 20 nm. (B) Nephrotoxicity of CDDP and NC-6004 in rats. The CDDP 10 mg/kg administration group showed significantly higher concentrations of blood urea nitrogen (BUN) and creatinine as compared with the control group and with the NC6004 10 mg/kg administration group. (C) Neurotoxicity of CDDP and NC-6004 in rats. Rats were given 2 mg/kg of CDDP (■) or NC-6004 (□) twice a week, 11 administrations in total. Animals given NC-6004 showed no delay in sensory nerve conductive velocity (SNCV) as compared with the control (▯). On the other hand, animals given CDDP showed a significant delay in SNCV as compared with animals given NC-6004 (A). The analysis by inductively-coupled plasma–mass spectrometer revealed that sciatic nerve concentrations of platinum (Pt) in mice given CDDP were more than 2-fold higher than NC-6004 (b). $*P < 0.05$ NS: not significant.

suggesting remarkable stability compared with typical micelles from amphiphilic block copolymers.[22]

Preclinical study. NC-6004 showed a very long blood retention profile compared with CDDP. The $AUC_{0\text{-}t}$ and C_{max} values were significantly higher in animals given NC-6004 than in animals given CDDP, namely, 65-fold and 8-fold, respectively ($P < 0.001$ and $P < 0.001$, respectively). Regarding platinum accumulation in the tumor, platinum concentrations peaked at 10 min following CDDP administration and at 48 h following NC-6004 administration. The C_{max} in the tumor was 2.5-fold higher for NC-6004 than for CDDP ($P < 0.001$). Furthermore, the tumor AUC was 3.6-fold higher for NC-6004 than for CDDP (81.2 μg/mL/h and 22.6 μg/mL/h, respectively).[23]

In nude mice implanted with the human gastric cancer cell line MKN-45, NC-6004 administration groups (5 mg/kg of CDDP) showed no significant difference in tumor growth rate compared with CDDP administration groups. Regarding time-course changes in body weight change rate, the CDDP (5 mg/kg) administration group showed a significant decrease ($P < 0.001$) in body weight compared with the control group. On the other hand, the NC-6004 administration group showed no decrease in body weight compared with the control group (data not shown).

Regarding renal function, the CDDP (10 mg/kg) administration group showed significantly higher plasma concentrations of BUN and creatinine than the control group ($P < 0.05$ and $P < 0.001$, respectively) and NC-6004 (10 mg/kg) administration group ($P < 0.05$ and $P < 0.001$, respectively) (Fig. 3B).

In neurological examination, rats given NC-6004 showed no delay in sensory nerve conductive velocity (SNCV) compared with animals given 5% glucose. On the other hand, rats given CDDP showed a significant delay ($P < 0.05$) in SNCV compared with animals given NC-6004. Sciatic nerve concentrations of

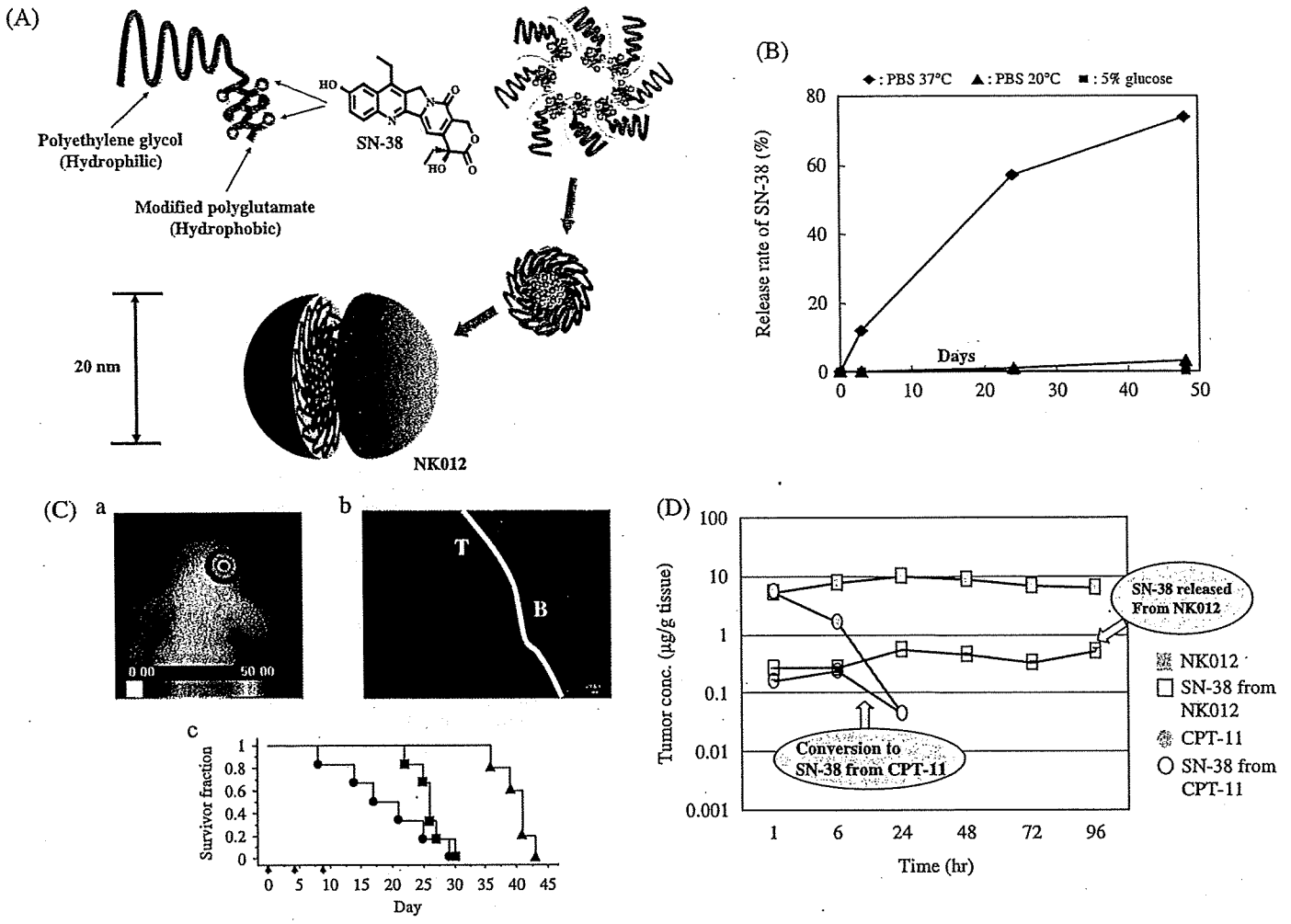

Fig. 4. (A) Schematic structure of NK012. A polymeric micelle carrier of NK012 consists of a block copolymer of polyethylene glycol (PEG) (molecular weight of ≈□5000) and partially modified polyglutamate (≈□ 20 units). Polyethylene glycol (hydrophilic) is believed to be the outer shell and SN-38 was incorporated into the inner core of the micelle. (B) The releasing rates of 7-ethyl-10-hydroxy-CPT (SN-38) from NK012. The data suggested that NK012 is stable in 5% glucose solution before administration and starts to release SN-38, gradually, under physiological conditions after administration. (C) (a) An orthotopic glioma model. Twenty days after U87MG/Luc inoculation. (b) The orthotopic tumor was visualized using a photon imager. The maximum tolerated dose (MTD) of NK012 (30 mg/kg) or Irinotecan hydrochloride (CPT-11) (66.7 mg/kg) was injected intravenously into the tail vein of mice. 24 h after NK012 injection, mice were also administered with fluorescein *Lycopersicon esculentum* lectin (100 μL/mouse) to visualize tumor blood vessels (green). NK012 (blue) was accumulated selectively in tumor tissue. T: tumor, B: normal brain (c) NK012 (30 mg/kg/day), CPT-11 (66.7 mg/kg/day) (■) and saline (●) were intravenously given on days 0 (20 days after tumor inoculation), 4, and 8 (▼). Kaplan-Meier analysis was performed to determine the effect of drugs on time to morbidity, and statistical differences were ranked according to the Mantel-Cox log-rank test using StatView 5.0. (D) Intra-tumor distribution of CPT-11, NK012 (or polymer bound SN-38), and free SN-38 after administration of NK012 and CPT-11 to mice bearing Capan1 xenografts. The time profiles of polymer-bound SN-38 (■), free SN-38 released from NK012 (□), CPT-11 (●), and free SN-38 converted from CPT-11 (○) were obtained by high performance liquid chromatography (HPLC) analysis. The time-points examined were 1, 6, 24, 48, 72, and 96 h after the administration of CPT-11 or NK012.

platinum were significantly ($P < 0.05$) lower in rats given NC-6004 (Fig. 3C). This finding is believed to be a factor that reduced neurotoxicity following NC-6004 administration compared with CDDP administration.

Clinical study. A phase I clinical trial of NC-6004 has recently been completed in the UK.[24] The starting dose of NC-6004 was 10 mg/m^2. NC-6004 was administered once every 3 weeks with only 1000 mL water loading at the day of administration. Administration of doses up to 120 mg/m^2 was performed without inducing significant nephrotoxicity. Although nausea and vomiting are typical CDDP adverse effects, those caused by NC-6004 were generally mild. However, hypersensitivity reactions caused by NC-6004 occurred more frequently than those caused by CDDP. A phase II study will soon be started involving sufficient anti-allergic premedication.

NK012: SN-38-incorporating micellar nanoparticle

Background. Irinotecan hydrochloride (CPT-11) has recently been demonstrated to be active against colorectal, lung, and ovarian cancers.[25–29] CPT-11 is a prodrug and is converted to 7-ethyl-10-hydroxy-CPT (SN-38), a biologically active metabolite of CPT-11, by carboxylesterases (CEs). SN-38 (Fig. 4A) is an analog of the plant alkaloid camptothecin which targets DNA topoisomerase I. SN-38 exhibits up to 1000-fold more potent cytotoxic activity against various cancer cells *in vitro* than CPT-11.[30] Although CPT-11 is converted to SN-38 in the liver and tumors, the metabolic conversion rate is less than 10% of the original volume of CPT-11.[31,32] Moreover, the conversion of CPT-11 to SN-38 depends on the genetic interindividual variability of CE activity.[33] Thus, further efficient use of SN-38 might be of great advantage and may be attractive for cancer

doi: 10.1111/j.1349-7006.2009.01103.x

treatment. The progress of the manufacturing technology of 'micellar nanoparticles' may make it possible to use SN-38 for *in vivo* experiments and further clinical use.

Preparation and characterization of NK012. NK012 is an SN-38-loaded polymeric micelle constructed in an aqueous milieu by the self-assembly of an amphiphilic block copolymer, PEG-PGlu(SN-38).[34] NK012 was obtained as a freeze-dried formulation and contained about 20% (w/w) of SN-38 (Fig. 4A). The mean particle size of NK012 is 20 nm in diameter with a relatively narrow range (Fig. 4A). The releasing rates of SN-38 from NK012 in phosphate buffered saline at 37°C were 57% and 74% at 24 h and 48 h, and those in 5% glucose solution at the same temperature and times were 1% and 3%, respectively (Fig. 4B). These results indicate that NK012 can release SN-38 under neutral conditions even without a hydrolytic enzyme, and is stable in 5% glucose solution. Thus, NK012 is suggested to be stable before administration and starts to release SN-38 gradually under physiological conditions following administration.

Preclinical study. Following CPT-11 injection, the plasma concentrations of CPT-11 and SN-38 rapidly decreased with time in a log-linear fashion. On the other hand, NK012 (polymer-bound SN-38) exhibited slower clearance. In tumor xenografts, NK012 clearance was significantly slower and free SN-38 concentration was maintained for a long time following injection.[34,35] Interestingly, there was no significant difference in the kinetic characteristics of free SN-38 in the small intestine between mice treated with NK012 and CPT-11.

Deviating from the ordinary experimental tumor model, tumors were allowed to grow until they became very large (approximately 1.5 cm), and then treatment was initiated. NK012 showed potent antitumor activity against bulky small cell lung cancer (SCLC) line, SBC-3/Neo, tumors compared with CPT-11. A striking antitumor activity was observed in mice treated with NK012 when we compared its antitumor activity with CPT-11 using SBC-3/VEGF (vascular endothelial growth factor) cells. In the clinical setting, CPT-11/5-FU (fluorouracil) combination therapy is now a standard regimen for colorectal cancer.[25,26] Therefore, it was speculated that the use of NK012 in place of CPT-11 in combination with 5-FU may yield superior results. As expected, the therapeutic effect of NK012/5-FU was significantly superior to that of CPT-11/5-FU against HT-29 xenografts ($P = 0.0004$)[36] (data not shown). In other tumors such as renal cancer,[37] glioma,[38] gastric cancer[39] and pancreatic cancer,[35] NK012 exerted significant superior antitumor activity and induced longer survival compared with CPT-11. In a glioma orthotopic xenograft model, both NK012 and CPT-11 appeared to be able to effectively extravasate from the blood–brain tumor barrier but not from normal brain vessels (Fig. 4C).[38] In a pancreatic cancer cell line, Capan-1 tumor xenograft as a hypovascular tumor model, it was also demonstrated that NK012 showed significantly more potent antitumor activity than CPT-11. Pharmacological examination revealed that only a slight conversion of SN-38 from CPT-11 was observed from 1 h to 24 h, and no SN-38 was detected thereafter. On the other hand, SN-38 released from NK012 continued to be detected from 1 h to 96 h following NK012 injection[35] (Fig. 4D).

Thus, NK012, which combines enhanced distribution with prolonged sustained release of SN-38 within tumors, is ideal for the treatment of hypovascular tumors since the antitumor activity of SN-38 is time-dependent.

Clinical study. Two independent phase I clinical trials have been conducted in the National Cancer Center in Japan[40] and the Sarah Canon Cancer Center in the US[41] in patients with advanced solid tumors to define the MTD, DLT, and recommended phase II dose. NK012 is infused intravenously over 60 min every 21 days until disease progression or unacceptable toxicity occurs. The MTD and RD were 37 mg/m^2 and 28 mg/m^2, respectively. DLT was neutropenia, and diarrhea was mild. The pharmacokinetics (PK) profile in the US study was similar to that in the Japanese study. Antitumor activity was also promising. Partial responses (PR)s were obtained in three patients with triple negative breast cancer, one patient with esophageal cancer and one patient with SCLC. A phase II study in patients with triple negative breast and colorectal cancers will soon be started in the US and Japan.

Future micelle formulations

The development of smart polymeric micelles that dynamically change their properties owing to their sensitivity to chemical or physical stimuli is the most promising trend, leading to the development of targeting therapy with high efficacy and ensured safety.[42] In this way, such micelles can respond to pathological or physiological endogenous stimuli already present in the body or to externally applied stimuli such as temperature, light or ultrasound. One sophisticated and rational formulation approach is to increase the hydrophobicity of the core of the polymeric micelles loaded with a platinum-based drug. This is to modulate the drug-releasing profile induced by chloride ion in the body fluid so as to have a sufficient induction period, and thus avoiding systemic drug leakage and achieving selective and sustained drug release at the site of a solid tumor.[43] Based on this strategy, dichloro (*trans*-l-1,2-diaminocyclohexane) platinum (II) (DachPt)-loaded micelles have recently been developed showing longer life in blood circulation and improved anticancer effects compared with cisplatin-loaded polymeric micelles (Fig. 5A).[44] A pH-triggered system also shows great promise in the treatment of intractable cancers. Here, the therapeutic agent should be stably associated with the hydrophobic core, and drug release is expected to occur with the destabilization of the micelle structure in response to an acidic pH of tumor tissue as well as with disruption of intracellular compartments such as the endosome and lysosome.[45] Notable antitumor efficacy against hypovascular cancer, including pancreatic and diffuse-type gastric cancers of doxorubicin-incorporating polymeric micelles with a pH-responding property was demonstrated to emphasize the promising application of DDS for the treatment of intractable cancers.[46] Photodynamic therapy, which involves the systemic administration of photosensitizers (PSs) and the subsequent photoirradiation of the diseased sites, is a promising physical approach for cancer treatment. However, PSs readily form aggregates, resulting in a significant reduction in singlet oxygen production. To prevent the self-quenching of PSs, ionic dendritic PSs (DPs) have been prepared and incorporated into polymeric micelles (Fig. 5B).[47] Eventually, the DP-loaded micelles showed a significant increase in photocytotoxicity compared with free DPs, achieving a remarkable photodynamic efficacy against a subcutaneous tumor model in experimental animals by systemic injection.

Success in gene and nucleic acid delivery indeed relies on the development of safe and effective carriers. In this regard, polyion complex (PIC) micelles, which are formed between nucleic acid and PEG-polycation block copolymers, have received much attention owing to their small size (~100 nm) and excellent biocompatibility.[48] Recently, an siRNA-incorporating PIC micelle has been prepared from the PEG-poly(lysine) block copolymer with sulthydryl (SH) groups in the side chain (Fig. 5C).[49] This PIC micelle is expected to release the loaded siRNA selectively in the cytoplasm by cleavage of disulfide cross-linking in response to a reductive intracellular environment, leading to the effective silencing of target genes related to oncogenesis. On the other hand, the disulfide cross-linking is sufficiently stable in the blood compartment, enabling prolonged circulation because of the oxidized atmosphere in the body. Furthermore, facilitated endosomal escape occurs in the PIC micelle having an intermediated layer between the shell and the core phase to exert selective destablization of the endosomal membrane through the proton

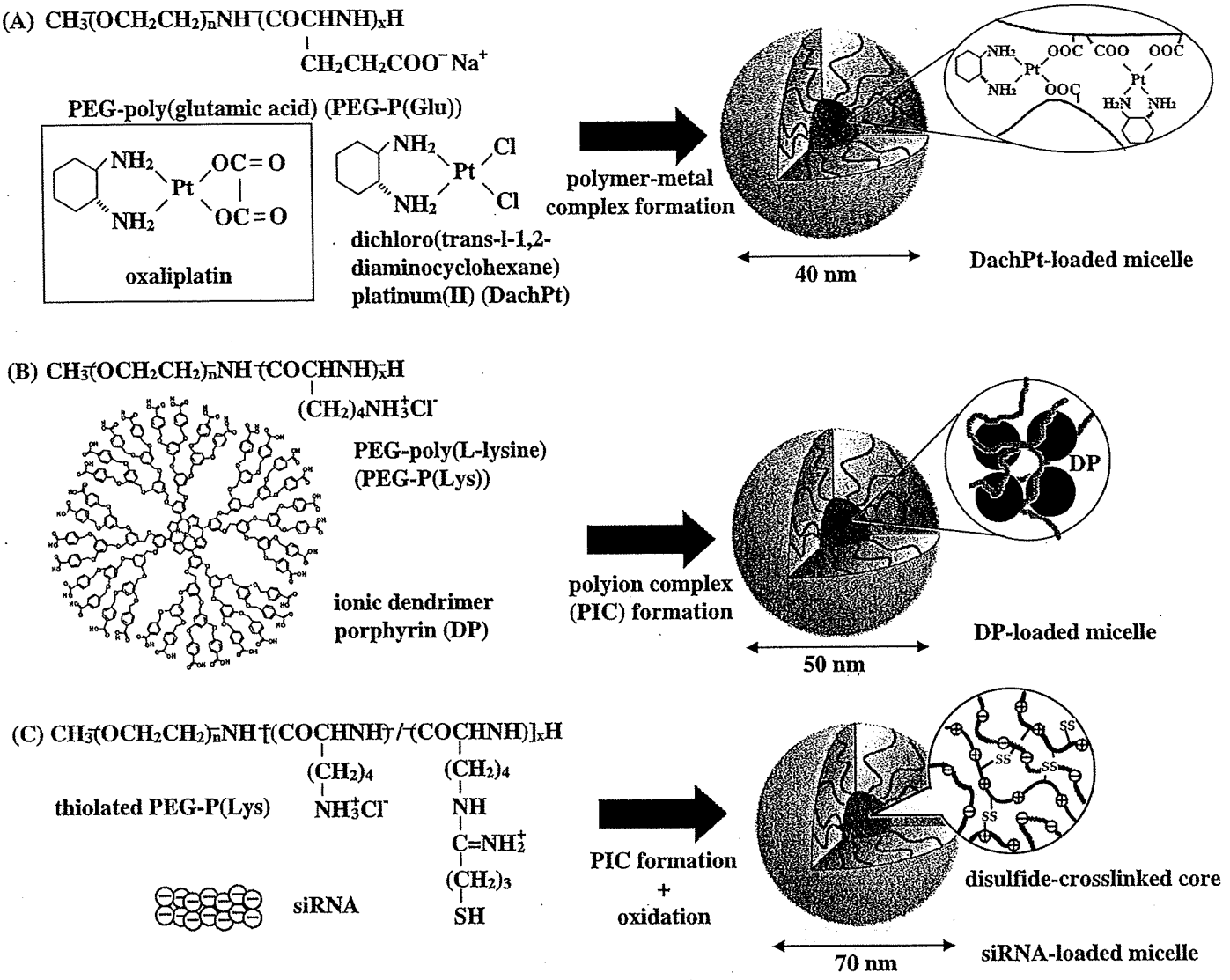

Fig. 5. Formation of polymeric micelles incorporating dichloro (*trans*-l-1,2-diaminocyclohexane) platinum (II) (DachPt) (A), ionic dendritic photosensitizers (B) and siRNA (C).

sponge effect as well as direct perturbation of the membrane structure.[50] The evaluation of these PIC micelles loaded with plasmid DNA or siRNA will soon be performed *in vivo* for future molecular therapy.

Conclusion

Presently, the phrase EPR proposed by Maeda *et al.* has become a fundamental principle in the field of DDS. Until recently, the EPR effect has not been recognized in the field of oncology; however, some oncologists have now become more acquainted with this effect since some drugs such as doxil, abraxane and several PEGylated proteinacious agents formulated based on the EPR effect have been approved in the field of oncology. Micelle carrier systems described here are obviously categorized as DDS based on the EPR effect. We believe that some anticancer agent-incorporating micelle nanoparticles may soon be approved for clinical use.

Acknowledgments

This work was supported by Third Term Comprehensive Control Research for Cancer from the Ministry of Health, Labour and Welfare of Japan, a Grant-in-Aid for Scientific Research or Priority Areas from the Ministry of Education, Culture, Sports, Science and Technology, and Japanese Foundation for Multidisciplinary Treatment of Cancer. We thank all researchers involved in this work and Ms. K Shiina for her secretarial support.

References

1 Matsumura Y, Maeda H. A new concept for macromolecular therapeutics in cancer chemotherapy: mechanism of tumoritropic accumulation of proteins and the antitumor agent smancs. *Cancer Res* 1986; **46**: 6387–92.
2 Maeda H, Wu J, Sawa T, Matsumura Y, Hori K. Tumor vascular permeability and the EPR effect in macromolecular therapeutics: a review. *J Contro Rel* 2000; **65**: 271–84.
3 Kataoka K, Kwon GS, Yokoyama M, Okano T, Sakurai Y. Block copolymer micelles as vehicles for drug delivery. *J Controlled Release* 1993; **24**: 119–32.
4 Yokoyama M, Miyauchi M, Yamada N *et al.* Polymer micelles as novel drug carrier: Adriamycin-conjugted poly (ethylene glycol)-poly (aspartic acid) block copolymer. *J Controlled Release* 1990; **11**: 269–78.
5 Yokoyama M, Okano T, Sakurai Y, Ekimoto H, Shibazaki C, Kataoka K. Toxicity and antitumor activity against solid tumors of micelle-forming

doi: 10.1111/j.1349-7006.2009.01103.x

polymeric anticancer drug and its extremely long circulation in blood. *Cancer Res* 1991; **51**: 3229–36.
6 Khayat D, Antoine EC, Coeffic D. Taxol in the management of cancers of the breast and the ovary. *Cancer Invest* 2000; **18**: 242–60.
7 Carney DN. Chemotherapy in the management of patients with inoperable non-small cell lung cancer. *Semin Oncol* 1996; **23**: 71–5.
8 Weiss RB, Donehower RC, Wiernik PH *et al.* Hypersensitivity reactions from taxol. *J Clin Oncol* 1990; **8**: 1263–8.
9 Rowinsky EK, Donehower RC. Paclitaxel (taxol). *N Engl J Med* 1995; **332**: 1004–14.
10 Rowinsky EK, Chaudhry V, Forastiere AA *et al.* Phase I and pharmacologic study of paclitaxel and cisplatin with granulocyte colony-stimulating factor: neuromuscular toxicity is dose-limiting. *J Clin Oncol* 1993; **11**: 2010–20.
11 Wasserheit C, Frazein A, Oratz R *et al.* Phase II trial of paclitaxel and cisplatin in women with advanced breast cancer: an active regimen with limiting neurotoxicity. *J Clin Oncol* 1996; **14**: 1993–9.
12 Hamaguchi T, Matsumura Y, Suzuki M *et al.* NK105, a paclitaxel-incorporating micellar nanoparticle formulation, can extend in vivo antitumour activity and reduce the neurotoxicity of paclitaxel. *Br J Cancer* 2005; **92**: 1240–6.
13 Hamaguchi T, Kato K, Matsumura Y *et al.* A Phase I and Pharmacokinetic Study of NK105, a Paclitaxel-incorporating Micellar Nanoparticle Formulation. *Br J Cancer* 2007; **97**: 170–6.
14 Horwich A, Sleijfer DT, Fossa SD *et al.* Randomized trial of bleomycin, etoposide, and cisplatin compared with bleomycin, etoposide, and carboplatin in good-prognosis metastatic nonseminomatous germ cell cancer: a Multiinstitutional Medical Research Council/European Organization for Research and Treatment of Cancer Trial. *J Clin Oncol* 1997; **15**: 1844–52.
15 Roth BJ. Chemotherapy for advanced bladder cancer. *Semin Oncol* 1996; **23**: 633–44.
16 Pinzani V, Bressolle F, Haug IJ, Galtier M, Blayac JP, Balmes P. Cisplatin-induced renal toxicity and toxicity-modulating strategies: a review. *Cancer Chemother Pharmacol* 1994; **35**: 1–9.
17 Cleare MJ, Hydes PC, Malerbi BW, Watkins DM. Anti-tumor platinum complexes. relationships between chemical properties and activity. *Biochimie* 1978; **60**: 835–50.
18 du Bois A, Luck HJ, Meier W *et al.* A randomized clinical trial of cisplatin/paclitaxel versus carboplatin/paclitaxel as first-line treatment of ovarian cancer. *J Natl Cancer Inst* 2003; **95**: 1320–9.
19 Cassidy J, Tabernero J, Twelves C *et al.* XELOX (capecitabine plus oxaliplatin): active first-line therapy for patients with metastatic colorectal cancer. *J Clin Oncol* 2004; **22**: 2084–91.
20 Horwich A, Sleijfer DT, Fossa SD *et al.* Randomized trial of bleomycin, etoposide, and cisplatin compared with bleomycin, etoposide, and carboplatin in good-prognosis metastatic nonseminomatous germ cell cancer: a Multi-institutional Medical Research Council/European Organization for Research and Treatment of Cancer Trial. *J Clin Oncol* 1997; **15**: 1844–52.
21 Bellmunt J, Ribas A, Eres N *et al.* Carboplatin-based versus cisplatin-based chemotherapy in the treatment of surgically incurable advanced bladder carcinoma. *Cancer* 1997; **80**: 1966–72.
22 Nishiyama N, Okazaki S, Matsumura Y *et al.* Novel cisplatin-incorporated polymeric micelles can eradicate solid tumors in mice. *Cancer Res* 2003; **63**: 8977–83.
23 Uchino H, Matsumura Y, Negishi T *et al.* Cisplatin-incorporating polymeric micelles (NC-6004) can reduce nephrotoxicity and neurotoxicity of cisplatin in rats. *Br J Cancer* 2005; **93**: 678–87.
24 Wilson RH, Plummer R, Adam J *et al.* Phase I and pharmacokinetic study of NC-6004, a new platinum entity of cisplatin-conjugated polymer forming micelles. *Am Soc Clin Oncol* 2008; (Abstract# 2573).
25 Saltz LB, Cox JV, Blanke C *et al.* Irinotecan plus fluorouracil and leucovorin for metastatic colorectal cancer. *Irinotecan Study Group N Engl J Med* 2000; **343**: 905–14.
26 Douillard JY, Cunningham D, Roth AD *et al.* Irinotecan combined with fluorouracil compared with fluorouracil alone as first-line treatment for metastatic colorectal cancer: a multicentre randomised trial. *Lancet* 2000; **355**: 1041–7.
27 Noda K, Nishiwaki Y, Kawahara M *et al.* Irinotecan plus cisplatin compared with etoposide plus cisplatin for extensive small-cell lung cancer. *N Engl J Med* 2002; **346**: 85–91.
28 Negoro S, Masuda N, Takada Y *et al.* CPT-11 Lung Cancer Study Group West. Randomised phase III trial of irinotecan combined with cisplatin for advanced non-small-cell lung cancer. *Br J Cancer* 2003; **88**: 335–41.
29 Bodurka DC, Levenback C, Wolf JK *et al.* Phase II trial of irinotecan in patients with metastatic epithelial ovarian cancer or peritoneal cancer. *J Clin Oncol* 2003; **21**: 291–7.
30 Takimoto CH, Arbuck SG. Topoisomerase I targeting agents: the camptothecins. In: Chabner BA, Lango DL, eds. *Cancer Chemotherapy and Biotherapy: Principal and Practice*, 3rd edn. Philadelphia (PA): Lippincott Williams & Wilkins, 2001: 579–646.
31 Slatter JG, Schaaf LJ, Sams JP *et al.* Pharmacokinetics, metabolism, and excretion of irinotecan (CPT-11) following I.V. infusion of [(14) C]CPT-11 in cancer patients. *Drug Metab Dispos* 2000; **28**: 423–33.
32 Rothenberg ML, Kuhn JG, Burris HA 3rd *et al.* Phase I and pharmacokinetic trial of weekly CPT-11. *J Clin Oncol* 1993; **11**: 2194–204.
33 Guichard S, Terret C, Hennebelle I *et al.* CPT-11 converting carboxylesterase and topoisomerase activities in tumor and normal colon and liver tissues. *Br J Cancer* 1999; **80**: 364–70.
34 Koizumi F, Kitagawa M, Negishi T *et al.* Novel SN-38-incorporating polymeric micelles, NK012, eradicate vascular endothelial growth factor-secreting bulky tumors. *Cancer Res* 2006; **66**: 10048–56.
35 Saito Y, Yasunaga M, Kuroda J, Koga Y, Matsumura Y. Enhanced distribution of NK012 and prolonged sustained-release of SN-38 within tumors are the key strategic point for a hypovascular tumor. *Caner Sci* 2008; **99**: 1258–64.
36 Nakajima T, Yasunaga Matsumura Y *et al.* Syneragistic antitumor activity of the novel SN-38 incorporating polymeric micelles, NK012, combined with 5-fluorouracil in a mouse model of colorectal cancer, as compared with that of irinotecan plus 5-fluorouracil. *Int J Cancer* 2008; **122**: 22148–53.
37 Sumitomo M, Koizumi F, Asano T *et al.* Novel SN-38-incorparated polymeric micelles, NK012, strongly supperss renal cancer progression. *Cancer Res* 2008, 2008; **122**: 2148–53.
38 Kuroda J, Kuratsu J, Yasunaga M, Koga Y, Matsumura Y. Potent antitumor effect of SN-38-incorporating polymeric micelle, NK012, against malignant glioma. *Int J Cancer* 2009; in press.
39 Nakajima-Eguchi T, Yanagihara K *et al.* Antitumor effect of SN-38-releasing polymeric micelles, NK012, on spontaneous peritoneal metastases from orthotopic gastoric cancer in mice sompared with irinotecan. *Caner Res* 2008; in press.
40 Kato K, Hamaguchi T, Shirao K *et al.* PhaseI study of NK012, polymer micelle SN-38, in patients with advanced cancer. *Proc Ams Soc Clin Oncol GI* 2008; (Abstract#485).
41 Burris IIIHA, Infante JR, Spigel DR *et al.* A phaseI dose-escalation study of NK012. *Proc Am Soc Clin Oncol* 2008; (Abstract#2538).
42 Nishiyama N, Kataoka K. Current state, achievements, and future prospects of polymeric micelles as nanocarriers for drug and gene delivery. *Pharmacol Ther* 2006; **112** (3): 630–48.
43 Cabral H, Nishiyama N, Okazaki S, Koyama H, Kataoka K. Preparation and biological properties of dichloro (1,2-diaminocyclohexane) platinum (II) (DACHPt)-loaded polymeric micelles. *J Control Release* 2005; **101** (1–3): 223–32.
44 Cabral H, Nishiyama N, Kataoka K. Optimization of (1,2-diamino-cyclohexane) platinum (II)-loaded polymeric micelles directed to improved tumor targeting and enhanced antitumor activity. *J Control Release* 2007; **121** (3): 146–55.
45 Bae Y, Fukushima S, Harada A, Kataoka K. Design of environment-sensitive supramolecular assemblies for intracellular drug delivery: polymeric micelles that are responsive to intracellular pH change. *Angew Chem Int Ed* 2003; **42** (38): 4640–3.
46 Kano MR, Bae Y, Iwata C *et al.* Improvement of cancer-targeting therapy, using nanocarriers for intractable solid tumors by inhibition of TGF-beta signaling. *P Natl Acad Sci USA* 2007; **104** (9): 3460–5.
47 Stapert HR, Nishiyama N, Jiang D-L, Aida T, Kataoka K. Polyion complex micelles encapsulating light-harvesting ionic dendrimer zinc porphyrins. *Langmuir* 2000; **16** (21): 8182–8.
48 Kataoka K, Togawa H, Harada A, Yasugi K, Matsumoto T, Katayose S. Spontaneous formation of polyion complex micelles with narrow distribution from antisense oligonucleotide and cationic block copolymer in physiological saline. *Macromolecules* 1996; **29** (26): 8556–7.
49 Matsumoto S, Christie RJ, Nishiyama N *et al.* Environment-responsive block copolymer micelles with a disulfide cross-linked core for enhanced siRNA delivery. *Biomaromolecules* in press.
50 Miyata K, Oba M, Kano MR *et al.* Polyplex micelles from triblock copolymers composed of tandemly aligned segments with biocompatible, endosomal escaping, and DNA-condensing functions for systemic gene delivery to pancreatic tumor. *Pharm. Res* in press.

Drugs of the Future 2009, 34(4): 276-281

CCC: 0377-8282/2009
DOI: 10.1358/dof.2009.34.4.1362406

MONOGRAPH

NK012

Apoptosis Inducer
Oncolytic

Nanosized-micellar particle containing 7-ethyl-10-hydroxycamptothecin (EHC), consisting of poly(ethylene glycol)-poly(glutamic acid)block copolymer chemically bound to EHC

EN: 417411

ABSTRACT

Selective tumor targeting by therapeutic agents is a long-standing pharmacological goal to improve selectivity and therapeutic indices. Most scientists have sought to use active receptor-mediated tumor-targeting systems, although the passive targeting afforded by the enhanced permeability and retention (EPR) effect provides a versatile and nonsaturable opportunity for tumor-selective delivery. Polymeric micelles are ideally suited to exploit the EPR effect, and they have been used for the delivery of a range of anticancer drugs in preclinical and clinical studies. NK012 is an SN-38-loaded polymeric micelle constructed in an aqueous milieu by the self-assembly of an amphiphilic block copolymer, PEG-PGlu(SN-38). Recently, we have demonstrated that NK012 exerts significantly more potent antitumor activity against various human tumor xenografts than irinotecan (CPT-11). Preclinical and clinical studies of NK012 up to the present are reviewed here.

BACKGROUND

Nanotechnology is one of the fastest moving technologies and is presently contributing significantly to the progress of medical science. Drugs categorized under the drug delivery system (DDS) are prepared primarily by utilizing nanotechnology. In the field of oncology, DDS drugs have been prepared and evaluated in preclinical and/or clinical trials, with some already approved for clinical use (Table I). More specifically, DDS can be used for active or passive targeting of tumor tissues. Active targeting refers to the development of monoclonal antibodies directed against tumor-related molecules, allowing targeting of a tumor from the specific binding of antibodies with respective antigens. However, the application of DDS using monoclonal antibodies is restricted to tumors expressing high levels of related antigens. Passive targeting can be achieved by utilizing the enhanced permeability and retention (EPR) effect (1, 2). This effect is based on the pathophysiological characteristics of solid tumor tissues, namely, hypervascularity, incomplete vascular architecture, secretion of vascular permeability factors stimulating extravasation within cancer tissue, and absence of effective lymphatic drainage from tumors that impedes the efficient clearance of macromolecules accumulated in solid tumor tissues (Fig. 1A, B).

Several techniques have been developed to maximally utilize the EPR effect, including modification of drug structures and the development of drug carriers. Polymeric micelle-based anticancer drugs were originally developed by Kataoka et al. in the late 1980s and early 1990s (3-5). Polymeric micelles were expected to increase the accumulation of drugs in tumor tissues by utilizing the EPR effect, as well as to incorporate various kinds of drugs into their inner core with relatively high stability by chemical conjugation or physical entrapment. Also, the size of micelles can be controlled within the diameter range of 20-100 nm to ensure that they do not penetrate normal vessel walls. With this development, it is expected that the incidence of drug-induced side effects may be decreased owing to reduced drug distribution in normal tissues.

Irinotecan hydrochloride (CPT-11) has been demonstrated to be active against colorectal, lung and ovarian cancers (6-10). CPT-11 is a prodrug that is converted to 7-ethyl-10-hydroxycamptothecin (SN-38, **1**), a biologically active metabolite of CPT-11, by carboxylesterases. SN-38 is an analogue of the plant alkaloid camptothecin, which targets DNA topoisomerase I. SN-38 exhibits up to 1,000-fold more potent cytotoxic activity against various cancer cells in vitro than CPT-11 (11). Although CPT-11 is converted to SN-38 in the liver and tumors, the metabolic conversion rate is less than 10% of the original volume of CPT-11 (12, 13). Moreover, the conversion of CPT-11 to SN-38 depends on the genetic interindividual variability of car-

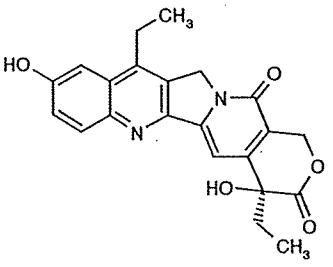

SN-38 (**1**)

Y. Matsumura.
Investigative Treatment Division, Research Centre for Innovative Oncology, National Cancer Center Hospital, Kashiwa, Japan. Correspondence: yhmatsum@east.ncc.go.jp

Table I. Examples of DDS in oncology and their stage of development.

Name	Platform	Compound	Clinical stage
Passive targeting			
NK-105	Micelles	Paclitaxel	II
NC-6004	Micelles	Cisplatin	I/II
NK012	Micelles	SN-38	II
Zinostatin stimalamer (SMANCS)	Polymer conjugate	Neocarzinostatin	Launched
Doxil	Liposome	Doxorubicin	Launched
Abraxane	Albumin-coated nanoparticle	Paclitaxel	Launched
Opaxio	Polymer conjugate	Paclitaxel	Prereg.
CT-2106	Polymer conjugate	Camptothecin	II
EndoTAG	Cationic liposome	Paclitaxel	II
Mureletecan	Polymer conjugate	Camptothecin	I
LE-SN-38	Liposome	SN-38	II
PK1	Polymer conjugate	Doxorubicin	II
IT-101	Polymer conjugate	Camptothecin	II
SP-1049C	Micelles	Doxorubicin	II
CPX-1	Liposome	CPT-11, floxuridine	II
Active targeting			
Mylotarg	Anti-CD33 antibody	Calicheamicin	Launched
Zevalin	Anti-CD20 antibody	90Y	Launched
Bexxar	Anti-CD20 antibody	131I	Launched
PK2	Galactose–polymer	Doxorubicin	I
MCC-465	Antibody liposome	Doxorubicin	I
MBP-426	Transferrin–liposome	Oxaliplatin	I
CALAA-01	Transferrin–polymer	siRNA	I
Trastuzumab-DM1	Anti-HER2 antibody	DM1	III

boxylesterase activity (14). Thus, further efficient use of SN-38 might be of great advantage and may be attractive for cancer treatment. The progress in the manufacturing technology of "micellar nanoparticles" may make it possible to use SN-38 for in vivo experiments and further clinical use.

NK012 is an SN-38-incorporating polymeric micelle that can accumulate selectively in solid tumor tissues utilizing the EPR effect. The micelle is constructed in an aqueous milieu by the self-assembly of an amphiphilic block copolymer, PEG-PGlu(SN-38) (15). NK012 was obtained as a freeze-dried formulation and contained about 20% (w/w) of SN-38. The mean particle size of NK012 is 20 nm in diameter, with a relatively narrow range (Fig. 2A). The release rates of SN-38 from NK012 in phosphate-buffered saline (PBS) at 37 °C were 57% and 74%, respectively, at 24 and 48 h, and in 5% glucose solution at the same temperature and times 1% and 3%, respectively (Fig. 2B). These results indicate that NK012 can release SN-38 under neutral conditions even without a hydrolytic enzyme, and is stable in 5% glucose solution. Thus, NK012 is suggested to be stable before administration and starts to release SN-38 gradually under physiological conditions following administration.

PRECLINICAL PHARMACOLOGY

Following CPT-11 injection, the plasma concentrations of CPT-11 and SN-38 rapidly decrease with time in a log-linear fashion. On the other hand, NK012 (polymer-bound SN-38) exhibited slower clearance. In tumor xenografts, NK012 clearance was significantly slower and the free SN-38 concentration was maintained for a long time following injection (15, 16). Interestingly, there was no significant difference in the kinetic characteristics of free SN-38 in the small intestine between mice treated with NK012 and CPT-11.

Deviating from the usual experimental tumor models, tumors were allowed to grow until they became very large (around 1.5 cm) and treatment was then initiated. NK012 showed potent antitumor activity against bulky small cell lung cancer SBC-3/Neo tumors compared with CPT-11. Striking antitumor activity was observed in mice treated with NK012 when its antitumor activity was compared with CPT-11 using SBC-3/VEGF cells. In the clinical setting, CPT-11/5-fluorouracil (5-FU) combination therapy is now a standard regimen for colorectal cancer (6, 7). It was therefore speculated that the use of NK012 in place of CPT-11 in combination with 5-FU might yield superior results. As expected, the therapeutic effect of NK012/5-FU was significantly superior to that of CPT-11/5-FU against human colon adenocarcinoma HT-29 xenografts (P = 0.0004) (17). In other tumors, such as renal cancer (18), glioma (19), gastric cancer (20) and pancreatic cancer (16), NK012 exerted significantly superior antitumor activity and was associated with longer survival compared with CPT-11. In an orthotopic glioma xenograft model, both NK012 and CPT-11 appeared to be able to effectively extravasate from the blood–brain tumor barrier but not from normal brain vessels (Fig. 2C) (19). In human pancreatic adenocarcinoma Capan-1 tumor xenografts, a hypovascular tumor model, it was also demonstrated that NK012 showed significantly more potent antitumor activity than CPT-11. Pharmacological examination revealed that only a slight conversion of SN-38 from CPT-11 was observed from 1 h to 24 h, and no SN-38 was detected thereafter. On the other hand, SN-38 released from NK012 continued to be detected from 1 h to 96 h fol-

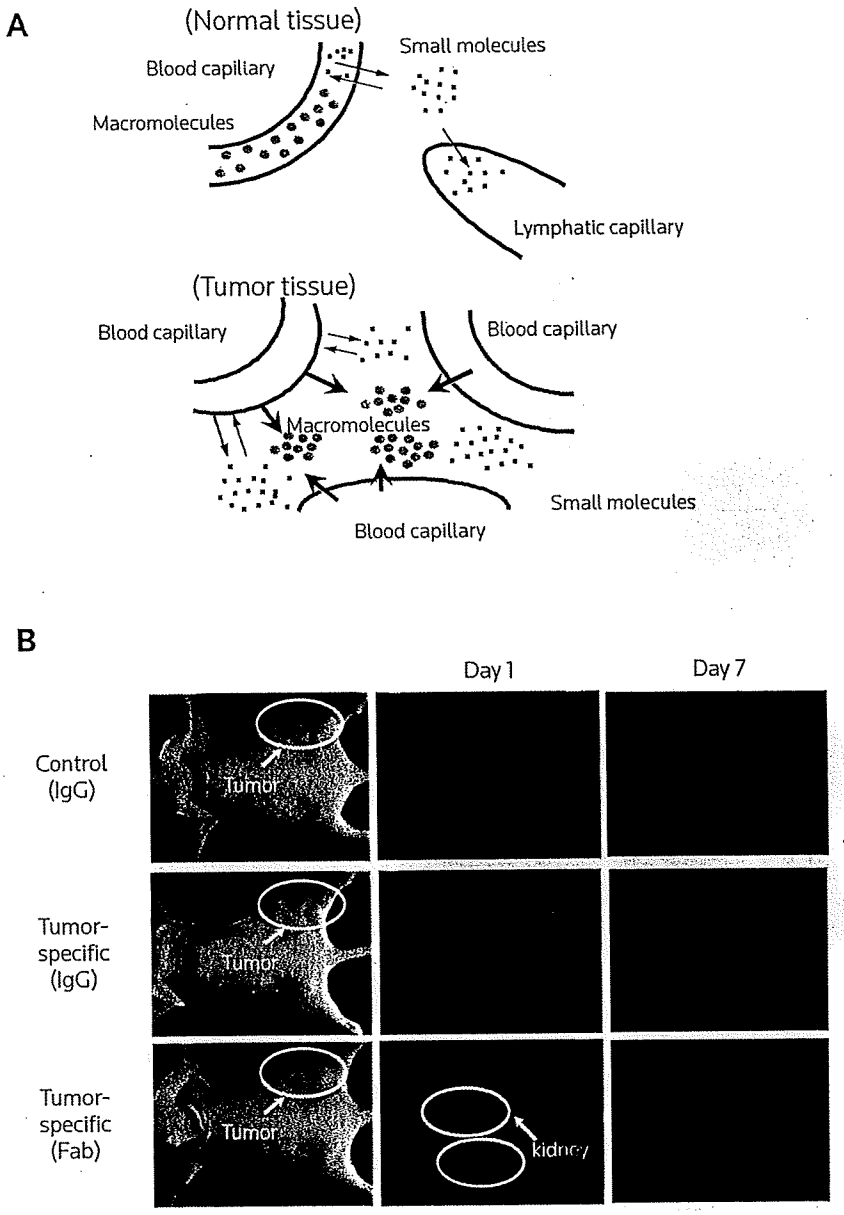

Figure 1. A. A diagram of normal and tumor tissue demonstrating the presence of a lymphatic duct in normal tissue (upper) but the absence of any lymphatic duct in tumor tissue (lower). Small molecules easily leak from normal vessels in the body, which endows them with a short plasma half-life. On the other hand, macromolecules have a long plasma half-life because they are too large to pass through the normal vessel walls, unless they are trapped by the reticuloendothelial system in various organs. In the solid tumor tissues shown in the lower panel, it was found that solid tumors generally possess several pathophysiological characteristics: hypervasculature, secretion of vascular permeability factors stimulating extravasation of macromolecules within the cancer, and absence of effective lymphatic drainage from tumors that impedes the efficient clearance of macromolecules accumulated in solid tumor tissues. These characteristics of solid tumors are the basis of the enhanced permeability and retention effect, or the EPR effect. **B.** In vivo imaging demonstrated that both control whole IgG and specific whole monoclonal antibody (mAb) accumulated selectively in the tumor tissue on day 1 after i.v. injection. On day 7, a greater degree of retention of the specific whole mAb as compared to the control IgG was noted. On the other hand, the F(ab) region of the specific mAb with a molecular weight of 50,000 accumulated in the tumor to the same extent as the control whole IgG. Interestingly, fluorescence of the F(ab) could also be detected in both kidneys, which implied that the F(ab) could easily pass through the kidney glomerulus. This accumulation of the control IgG in the tumor represents the EPR effect. The findings suggest that not only the specific affinity of the mAb, but also the size of the molecules and the stability of the molecules in blood, are important for tumor-selective targeting.

lowing NK012 injection (16) (Fig. 2D). Thus, NK012, which combines enhanced distribution with sustained release of SN-38 within tumors, is ideal for the treatment of hypovascular tumors since the antitumor activity of SN-38 is time-dependent.

CLINICAL STUDIES

Two independent phase I clinical trials have been conducted at the National Cancer Center in Japan (21) and the Sarah Cannon Cancer Center in the U.S. (22) in patients with advanced solid tumors to

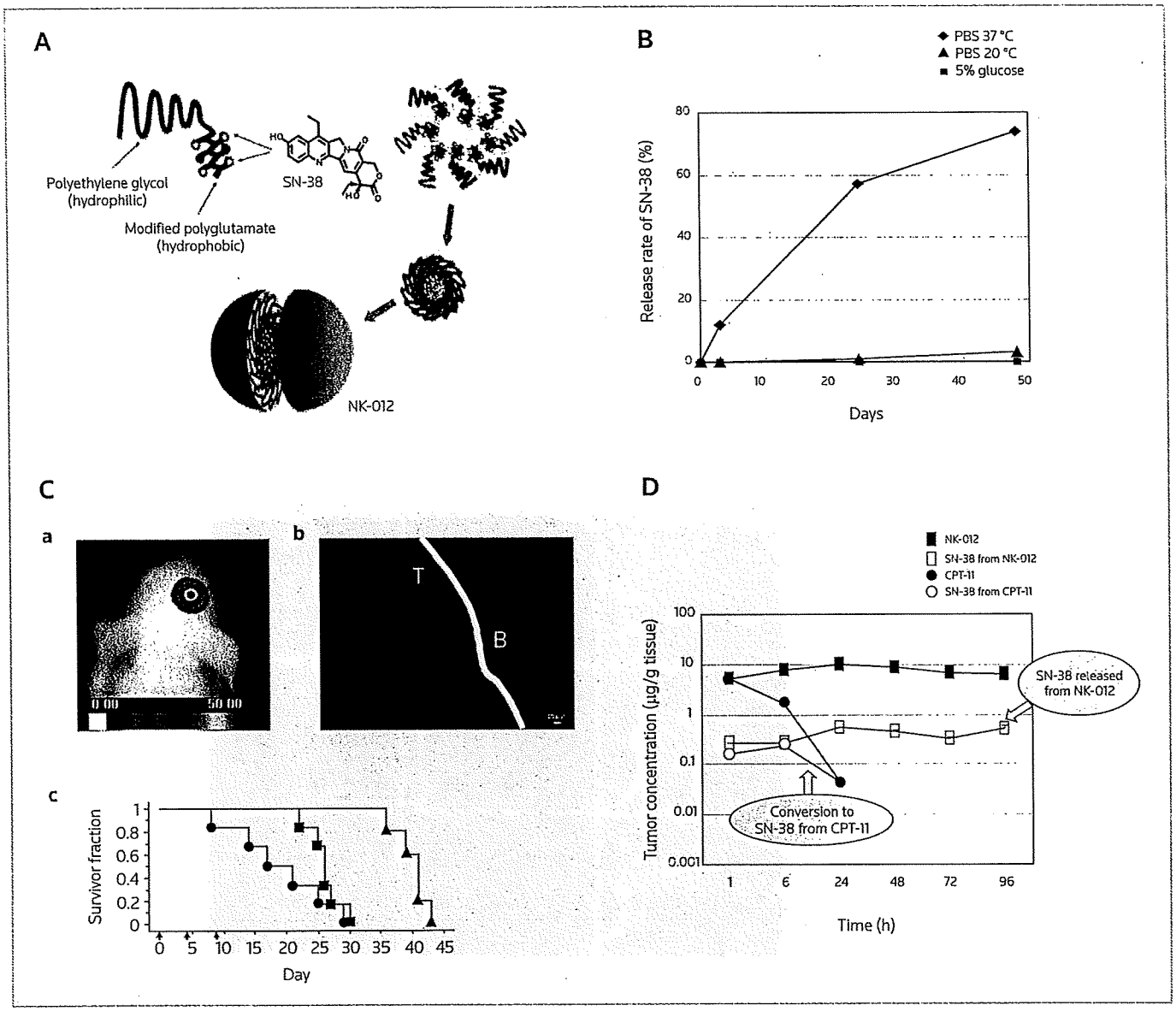

Figure 2. A. Schematic structure of NK012. A polymeric micelle carrier of NK012 consists of a block copolymer of polyethylene glycol (PEG; molecular weight of about 12,000) and partially modified polyglutamate (about 20 units). PEG (hydrophilic) is believed to be the outer shell and SN-38 is incorporated into the inner core of the micelle. **B.** The release rates of SN-38 from NK012 in phosphate-buffered saline (PBS) were 74% at 48 h but only 3% at 48 h in 5% glucose solution. It is therefore suggested that NK012 is stable in 5% glucose solution before administration and starts to release SN-38 gradually under physiological conditions after administration. **C. a)** An orthotopic glioma model. Twenty days after U-87 MG/Luc inoculation, the maximum tolerated dose (MTD) of NK012 (30 mg/kg) or CPT-11 (66.7 mg/kg) was injected i.v. into the tail vein of mice. **b)** 24 h after NK012 (blue) injection, mice were also administered fluorescein *Lycopersicon esculentum* lectin (100 μL/mouse) to visualize tumor-blood vessels. T, tumor, B, normal brain. **c)** NK012 (30 mg/kg/day), CPT-11 (66.7 mg/kg/day) (■) and saline (●) were given i.v. on days 0 (20 days after tumor inoculation), 4 and 8(▼). Kaplan–Meier analysis was performed to determine the effect of drugs on time to morbidity, and statistical differences were ranked according to the Mantel–Cox log-rank test using StatView 5.0. **D.** Tumor distribution of CPT-11, NK012 (or polymer-bound SN-38) and free SN-38 after administration of NK012 and CPT-11 to mice bearing human pancreatic adenocarcinoma Capan-1 **(a)** or PSN-1 **(b)** xenografts. The time profiles of polymer-bound SN-38 (■), free SN-38 released from NK012 (□), CPT-11 (●) and free SN-38 converted from CPT-11 (○) were obtained by high-performance liquid chromatographic (HPLC) analysis. The time points examined were 1, 6, 24, 48, 72 and 96 h after administration of CPT-11 or NK012.

define the maximum tolerated dose (MTD), dose-limiting toxicity (DLT) and recommended phase II dose. NK012 was infused i.v. over 30 min every 21 days until disease progression or unacceptable toxicity. The MTD was 37 mg/m^2 in the U.S. and 28 mg/m^2 in Japan. The recommended dose was the same (28 mg/m^2) in both countries. DLT was mostly neutropenia or related events, and diarrhea was mild. The pharmacokinetic profile in the U.S. study was similar to that in the Japanese study. Antitumor activity was also promising. Partial responses were obtained in three patients with triple-negative breast cancer, one patient with esophageal cancer, one patient with small cell lung cancer and one patient with lung carcinoid. Phase II studies in patients with triple-negative breast and colorectal cancers are being planned in the U.S. and Japan, respectively.

DISCLOSURE

This work was supported by Third Term Comprehensive Control Research for Cancer from the Ministry of Health, Labour and Welfare of Japan, a Grant-in-Aid for Scientific Research or Priority Areas from the Ministry of Education, Culture, Sports, Science and Technology, and Japanese Foundation for Multidisciplinary Treatment of Cancer and the Princess Takamatsu Cancer Research Fund (07-23908). The author declares no potential conflict of interest.

REFERENCES

1. Matsumura, Y., Maeda, H. *A new concept for macromolecular therapeutics in cancer chemotherapy: Mechanism of tumoritropic accumulation of proteins and the antitumor agent SMANCS.* Cancer Res 1986, 46(12, Pt. 1): 6387-92.
2. Maeda, H., Wu, J., Sawa, T., Matsumura, Y., Hori, K. *Tumor vascular permeability and the EPR effect in macromolecular therapeutics: A review.* J Control Release 2000, 65(1-2): 271-84.
3. Kataoka, K., Kwon, G.S., Yokoyama, M., Okano, T., Sakurai, Y. *Block copolymer micelles as vehicles for drug delivery.* J Control Release 1993, 24: 119-32.
4. Yokoyama, M., Miyauchi, M., Yamada, N. et al. *Polymer micelles as novel drug carrier: Adriamycin-conjugated poly(ethylene glycol)-poly(aspartic acid) block copolymer.* J Control Release 1990, 11: 269-78.
5. Yokoyama, M., Okano, T., Sakurai, Y., Ekimoto, H., Shibazaki, C., Kataoka, K. *Toxicity and antitumor activity against solid tumors of micelle-forming polymeric anticancer drug and its extremely long circulation in blood.* Cancer Res 1991, 51(12): 3229-36.
6. Saltz, L.B., Cox, J.V., Blanke, C. et al. *Irinotecan plus fluorouracil and leucovorin for metastatic colorectal cancer. Irinotecan Study Group.* N Engl J Med 2000, 343(13): 905-14.
7. Douillard, J.Y., Cunningham, D., Roth, A.D. et al. *Irinotecan combined with fluorouracil compared with fluorouracil alone as first-line treatment for metastatic colorectal cancer: A multicentre randomised trial.* Lancet 2000, 355(9209): 1041-7.
8. Noda, K., Nishiwaki, Y., Kawahara, M. et al. *Irinotecan plus cisplatin compared with etoposide plus cisplatin for extensive small-cell lung cancer.* N Engl J Med 2002, 346(2): 85-91.
9. Negoro, S., Masuda, N., Takada, Y. et al. *CPT-11 Lung Cancer Study Group West. Randomised phase III trial of irinotecan combined with cisplatin for advanced non-small-cell lung cancer.* Br J Cancer 2003, 88(3): 335-41.
10. Bodurka, D.C., Levenback, C., Wolf, J.K. et al. *Phase II trial of irinotecan in patients with metastatic epithelial ovarian cancer or peritoneal cancer.* J Clin Oncol 2003, 21(2): 291-7.
11. Takimoto, C.H., Arbuck, S.G. *Topoisomerase I targeting agents: The camptothecins.* In: Cancer Chemotherapy and Biotherapy: Principal and Practice, 3rd Ed. Chabner, B.A., Lango, D.L. (Eds.). Lippincott Williams & Wilkins: Philadelphia, 2001, 579-646.
12. Slatter, J.G., Schaaf, L.J., Sams, J.P. et al. *Pharmacokinetics, metabolism, and excretion of irinotecan (CPT-11) following I.V. infusion of [(14)C]CPT-11 in cancer patients.* Drug Metab Dispos 2000, 28(4): 423-33.
13. Rothenberg, M.L., Kuhn, J.G., Burris, H.A. 3rd et al. *Phase I and pharmacokinetic trial of weekly CPT-11.* J Clin Oncol 1993, 11(11): 2194-204.
14. Guichard, S., Terret, C., Hennebelle, I. et al. *CPT-11 converting carboxylesterase and topoisomerase activities in tumor and normal colon and liver tissues.* Br J Cancer 1999, 80(3-4): 364-70.
15. Koizumi, F., Kitagawa, M., Negishi, T. et al. *Novel SN-38-incorporating polymeric micelles, NK012, eradicate vascular endothelial growth factor-secreting bulky tumors.* Cancer Res 2006, 66(20): 10048-56.
16. Saito, Y., Yasunaga, M., Kuroda, J., Koga, Y., Matsumura, Y. *Enhanced distribution of NK012 and prolonged sustained-release of SN-38 within tumors are the key strategic point for a hypovascular tumor.* Cancer Sci 2008, 99(6): 1258-64.
17. Nakajima, T.E, Yasunaga, M., Kano, Y. et al. *Synergistic antitumor activity of the novel SN-38 incorporating polymeric micelles, NK012, combined with 5-fluorouracil in a mouse model of colorectal cancer, as compared with that of irinotecan plus 5-fluorouracil.* Int J Cancer 2008, 122(9): 2148-53.
18. Sumitomo, M., Koizumi, F., Asano, T. et al. *Novel SN-38-incorporated polymeric micelle, NK012, strongly suppresses renal cancer progression.* Cancer Res 2008, 68(6): 1631-5.
19. Kuroda, J., Kuratsu, J., Yasunaga, M., Koga, Y., Matsumura, Y. *Potent antitumor effect of SN-38-incorporating polymeric micelle, NK012, against malignant glioma.* Int J Cancer 2009, 124(11): 2505-11.
20. Nakajima, T.E., Yanagihara, K., Takigahira, M. et al. *Antitumor effect of SN-38-releasing polymeric micelles, NK012, on spontaneous peritoneal metastases from orthotopic gastric cancer in mice compared with irinotecan.* Cancer Res 2008, 68(22): 9318-22.
21. Toshihiko, D., Fuse, N., Ohtsu, A. et al. *A phase I dose escalation study of NK012, polymer micelle of irinotecan metabolite SN-38, in patients with advanced cancer.* Eur J Cancer Suppl [20th EORTC-NCI-AACR Symp Mol Targets Cancer Ther (Oct 21-24, Geneva) 2008] 2008, 6(12): Abst 423.
22. Burris, H.A. III, Infante, J.R., Spigel, D.R. et al. *A phase I dose-escalation study of NK012.* Proc Am Soc Clin Oncol [44th Annu Meet Am Soc Clin Oncol (ASCO) (May 30-June 3, Chicago) 2008] 2008, 26(15, Suppl.): Abst 2538.

ADDITIONAL REFERENCES

Onda, T., Mashiba, H., Seno, C. et al. *Sequence-dependent combination effect of NK012, a novel micellar nanoparticle of SN-38, with 5-fluorouracil in mouse colon cancer model.* Proc Am Assoc Cancer Res (AACR) 2008, 49: Abst 5626.

Matsumoto, S.-I., Goda, R., Onda, T. et al. *NK012, SN-38-incorporating micellar nanoparticle, improves tumor disposition of SN-38 and elicits superior antitumor activity to irinotecan.* Proc Am Assoc Cancer Res (AACR) 2008, 49: Abst 5627.

Nakajima, T.E., Yanagihara, K., Takigahira, M. et al. *Antitumor activity of polymeric micelles incorporating SN-38 (NK012) in mouse models of orthotopically planted gastric carcinoma progressing peritoneal dissemination.* Proc Am Assoc Cancer Res (AACR) 2008, 49: Abst LB-109.

Kato, K., Hamaguchi, T., Shirao, K. et al. *Interim analysis of phase I study of NK012, polymer micelle SN-38, in patients with advanced cancer.* Gastrointest Cancers Symp (Jan 25-27, Orlando) 2008, Abst 485.

Onda, T., Ichimura, E., Matsumoto, S.-I., Okamoto, K., Nishikawa, K. *Marked anti-tumor activity of NK012, 7-ethyl-10-hydroxycamptothecin-incorporating micellar nanoparticle, in liver metastatic tumor model of colorectal cancer.* Proc Am Assoc Cancer Res (AACR) 2007, 48: Abst 1495.

Nakajima, T., Matsumura, Y., Koizumi, F. et al. *Synergistic anti-tumor activity of novel polymeric micelles incorporating SN-38 (NK012) in combination with 5-fluorouracil (5-FU) in mouse model of colon cancer.* Proc Am Assoc Cancer Res (AACR) 2007, 48: Abst 4729.

Sumitomo, M., Kuroda, K., Koizumi, F. et al. *Novel SN-38-incorporating polymeric micelles, NK012, eradicate bulky renal tumors.* J Urol 2007, 177(4, Suppl.): Abst 312.

Saito, Y., Yasunaga, M., Matsumura, Y. *NK012, SN-38-incorporating micelles can eradicate pancreatic solid tumor with abundant stroma.* 66th Annu Meet Jpn Cancer Assoc (Oct 3-5, Yokohama) 2007, Abst O-447.

Onda, T., Nakamura, I., Ichimura, E. et al. *Micellar NK012 drastically improves intratumoral SN-38-delivery and elicits superior anti-tumor activity to irinotecan.* 66th Annu Meet Jpn Cancer Assoc (Oct 3-5, Yokohama) 2007, Abst P-1275.

Okamoto, K., Seno, C., Nakamura, I., Onda, T., Nishikawa, K. *Synergistic anti-tumor activity of NK012, SN-38-incorporating micellar nanoparticles, in combination with bevacizumab.* 66th Annu Meet Jpn Cancer Assoc (Oct 3-5, Yokohama) 2007, Abst P-1277.

Onda, T., Nakamura, I., Seno, C. et al. *Superior antitumor activity of NK012, 7-ethyl-10-hydroxycamptothecin-incorproating micellar nanoparticle, to irinotecan.* Proc Am Assoc Cancer Res (AACR) 2006, 47: Abst 3062.

Koizumi, F., Matsumura, Y. *Novel SN-38-incorporating polymeric micelles, NK012 eradicate vascular endothelial growth factor-secreting bulky tumors.* Proc Am Assoc Cancer Res (AACR) 2006, 47: Abst 3063.

Int. J. Cancer: **124,** 2505–2511 (2009)

FAST TRACK

Potent antitumor effect of SN-38-incorporating polymeric micelle, NK012, against malignant glioma

Jun-ichiro Kuroda[1,2], Jun-ichi Kuratsu[2], Masahiro Yasunaga[1], Yoshikatsu Koga[1], Yohei Saito[1] and Yasuhiro Matsumura[1]*

[1]*Investigative Treatment Division, Research Center for Innovative Oncology, National Cancer Center Hospital East, Kashiwa, Japan*
[2]*Department of Neurosurgery, Faculty of Medical and Pharmaceutical Sciences, Kumamoto University, Kumamoto, Japan*

Recent published reports on clinical trials of CPT-11 indicate the effectiveness of this compound, a prodrug of SN-38, against malignant glioma in combination with anti-vascular endothelial growth factor antibody. Here, we determined if NK012, and SN-38 incorporating micelle, can be an appropriate formulation for glioblastoma treatment compared with CPT-11. *In vitro* cytotoxicity was evaluated against several glioma lines with NK012, CPT-11, SN-38, ACNU, CDDP and etoposide. For the *in vivo* test, a human glioma line (U87MG) transfected with the *luciferase* gene was inoculated into nude mice brain for pharmacokinetic analysis by fluorescence microscopy and high-performance liquid chromatography after intravenous injection of NK012 and CPT-11. *In vivo* antitumor activity of NK012 and CPT-11 was evaluated by bioluminescence image and Kaplan-Meier analyses. The growth-inhibitory effects of NK012 were 34- to 444-fold more potent than those of CPT-11. Markedly enhanced and prolonged distribution of free SN-38 in the xenografts was observed after NK012 injection compared with CPT-11. NK012 showed significantly potent antitumor activity against an orthotopic glioblastoma multiforme xenograft and significantly longer survival rate than CPT-11 ($p = 0.0014$). This implies that NK012 can pass through the blood brain tumor barrier effectively. NK012, which combines enhanced distribution with prolonged sustained release, may be ideal for glioma treatment. Currently, a phase I study of NK012 is almost complete in Japan and the US. The present translational study warrants the clinical phase II study of NK012 in patients with malignant glioma.

Key words: glioma; drug delivery system; blood brain barrier (BBB); SN-38; micelles

Malignant astrocytomas, such as anaplastic astrocytoma and glioblastoma multiforme (GBM), are the most common and highly vascularized glial tumors of the brain. At least 80 percent of malignant gliomas are categorized as GBM.[1] Currently, GBM patients have a mean survival of only 50 weeks following the standard treatment consisting of surgical and adjuvant therapies.[2] A recent phase III randomized trial for newly diagnosed GBM demonstrated that radiation therapy with concurrent temozolomide treatment, followed by 6 months of temozolomide treatment was superior to radiation therapy alone in terms of overall survival.[3] In addition, several clinical trials have demonstrated that the median survival times of patients with recurrence were only 3–6 months.[4]

The anticancer plant alkaloid 7-ethyl-10-hydroxy-camptothecine (SN-38) is a broad spectrum anticancer agent targeting DNA topoisomerase I with a different mechanism of action compared with alkylating agents such as temozolomide. Although SN-38 has shown promising anticancer activity *in vitro* and *in vivo*, its clinical application has remained dormant because of its low therapeutic efficacy and severe toxic effects.[5,6] Irinotecan hydrochloride (CPT-11), a prodrug of SN-38, shows some antitumor activities in patient with recurrent GBM, with response rates of 0 to 17% in several trials.[7–10] CPT-11 activity is thus similar to that of other agents used for recurrent GBM.[9] A recent phase II trial for recurrent GBM demonstrated that the combination of CPT-11 and bevacizumab, an antivascular endothelial growth factor (VEGF) monoclonal antibody, is an effective treatment against the neoplasia with a 6-month progression-free survival rate of 46% and a 6-month overall survival rate of 77%.[11,12] However, there is an increased risk of developing venous thromboembolic disease and intracranial hemorrhage with this combination therapy. Therefore, there is an urgent need to develop treatment modalities by which cytotoxic drugs can exert more potent antitumor activity to their full potential with modest adverse effects and thereby reasonably prolong the overall survival in GBM patients.

The purpose of the drug delivery system (DDS) is to achieve selective delivery of antitumor agents to tumor tissue at an effective concentration for the appropriate duration of time in order to reduce the adverse effects of the administered drug and simultaneously enhance its antitumor effect. There are 2 main concepts in DDS, active targeting and passive targeting. Active targeting involves a monoclonal antibody and a ligand to a tumor-related receptor. Doxil, a doxorubicine incorporated polyethylene glycol conjugated liposome, is categorized under passive targeting agents and are already in clinical use.[13,14] NK012, a novel SN-38-incorporating polymeric micelle, is a prodrug of SN-38 similar to CPT-11 and categorized under passive targeting agent as well. Although CPT-11 is converted to SN-38 in tumors by carboxylesterase (CE), the metabolic conversion rate is within 2–8% of the original volume of CPT-11.[15,16] In contrast, the release rate of SN-38 from NK012 is 74% under physiologic pH condition even without CEs.[17] Recently, we have demonstrated that NK012 exerted significantly more potent antitumor activity against various human tumor xenografts than CPT-11.[17–20] However, there is a fundamental question whether such nanoparticles can reach brain tumors across the tumor microvessels. In the present study, therefore, we established an orthotopic glioma model in this experiment and then evaluated whether NK012 can pass through the BTB and exert its antitumor effect on orthotopic human glioma xenografts in comparison with CPT-11.

Material and methods

Drugs

NK012 and SN-38 were donated by Nippon Kayaku Co., Ltd. (Tokyo, Japan). The size of NK012 was ~20 nm in diameter with a narrow size distribution.[17] ACNU [1-(4-amino-2-methyl-5-pyrimidinyl) methyl-3-(2-chloroethyl)-3-nitrosourea, nimstine] was purchased from DAIICHI SANKYO Co., Ltd. (Tokyo, Japan). CDDP (cis-diamminedichloroplatinum) and CPT-11 were purchased from Yakult Co., Ltd. (Tokyo, Japan). Etoposide [4′demethlepipodophyllotoxin-9-(4, 6-O-ethylidene-β-D-glucopyranoside)] was purchased from BIOMOL (Plymouth Meeting, PA).

Grant sponsors: Ministry of Health, Labour and Welfare of Japan (Third Term Comprehensive Contorol Research for Cancer), Core Research for Evolutional Science and Technology, Ministry of Education, Culture, Sports, Science and Technology.

***Correspondence to:** Investigative Treatment Division, Research Center for Innovative Oncology, National Cancer Center Hospital East, 6-5-1 Kashiwanoha, Kashiwa 277-8577, Japan. Fax: +81-4-7134-6857.
E-mail: yhmatsum@east.ncc.go.jp.

Received 10 September 2008; Accepted after revision 28 October 2008
DOI 10.1002/ijc.24171
Published online 24 November 2008 in Wiley InterScience (www.interscience.wiley.com).

Cells and animals

Five human glioma cell lines, namely U87MG, U251MG, U118MG, LN18 and LN229, were obtained from the American Type Culture Collection (Rockville, MD). Cells were maintained in Dulbecco's modified Eagle's minimum essential medium supplemented with 10% fetal bovine serum (Cell Culture Technologies, Gaggenau-Hoerden, Germany), penicillin, streptomycin and amphotericin B (100 units/ml, 100 μg/ml and 25 μg/ml, respectively; Sigma, St. Louis, MO) in a humidified atmosphere containing 5% CO_2 at 37°C. Six- to eight-week-old athymic nude mice (nu/nu; Charles River Japan, Kanagawa, Japan) were used for this study. U87MG cells (1×10^5) were injected into the cerebral hemisphere using a Hamilton syringe through an entry point 1 mm anterior and 1.8 mm lateral to the bregma to an intraparenchymal depth of 2.5 mm. The rate of injection was 0.5 μl/min, and the needle was left in place for 5 min after completion of the injection. All animal procedures were performed in compliance with the Guidelines for the Care and Use of Experimental Animals established by the Committee for Animal Experimentation of the National Cancer Center, Japan; these guidelines meet the ethical standards required by law and also comply with the guidelines for the use of experimental animals in Japan.

Establishment of U87MG cell line stably expressing firefly luciferase and YFP mutant Venus

For the *in vivo* bioluminescence imaging of orthotopic brain tumors, the U87MG cell line stably expressing firefly luciferase and the YFP mutant Venus was established. Briefly, the coding sequence for firefly luciferase and Venus was subcloned into the the pIRES Vector (Clontech Laboratories, Mountain View, CA). The fragment consists of Luciferase-IRES-Venus generated from the plasmid with the restriction enzymes Nhe I and Not I. This fragment was subcloned into the pEF6/V5-His Vector (Invitrogen, Carlsbad, CA) to generate plasmids of pEF6-Lucifease IRES Venus. U87MG cells (2×10^6) were seeded onto 10-cm dishes 24 hr before transfection. The cells were transfected with 10 μg of pEF6-Lucifease IRES Venus using FuGENE HD Transfection Reagent (Roche Diagnostics, Mannheim, Germany) according to manufacturer's instructions, and then incubated for 48 hr at 37°C. The cells were then passaged in medium containing Blasticidin (10 μg/ml; InvivoGen, San Diego, CA) to select for the Blasticidin resistance gene integrated in the pEF6/V5-His plasmids. Venus expression was used as a surrogate marker of luciferase-positive cells. Venus-expressing U87MG cells (U87MG/Luc) were sorted using the BD FACS Aria cell sorter (BD Biosciences, San Jose, CA), and expanded in selection medium. The accuracy of a quantitive bioluminescence image as an indicator of U87MG/Luc cell number was analyzed using the Photon Imager animal imaging system *in vitro*, as described under *in vivo* growth inhibition assay. This analysis demonstrated clear correlation between a quantitive bioluminescence image and cell number ($R^2 = 0.99$). The sensitivity of U87MG/Luc cells to each drug (NK012, CPT-11, SN-38, ACNU, CDDP and etoposide) was almost similar to that of parental U87MG cells (data not shown).

In vitro *growth inhibition assay*

Cell growth inhibition was measured by the tetrazolium salt-based proliferation assay (WST assay; Wako Chemicals, Osaka, Japan). Briefly, cells (5×10^3 cells/well) in 96-well plates were incubated overnight. Then, growth medium was changed to new medium with various concentrations of SN-38, NK012, CPT-11, ACNU, etoposide and CDDP. After 72 hr of incubation, medium was changed to new medium containing 10% WST-8 reagents. After 1 hr of incubation, the absorbance of the formazan product formed was detected at 450 nm in a 96-well spectrophotometric plate reader (SpectraMax 190; Molecular Devices, Sunnyvale, CA). Cell viability was measured and compared with that of the control cells. Each experiment was carried out in triplicates and was repeated at least 3 times. Data were averaged and normalized against the nontreated controls to generate dose-response curves. The number of living cells (% Control) was calculated using the following formula: % Control = (each absorbance—absorbance of blank well)/absorbance of control well × 100.

Evaluation of NK012 and CPT-11 distribution in tumor tissue by fluorescence microscopy

The U87MG orthotopic xenograft model described earlier was used for the analysis of the biodistribution of NK012 and CPT-11. Twenty days after U87MG/Luc inoculation, the maximum tolerated dose (MTD) of NK012 (30 mg/kg) or CPT-11 (66.7 mg/kg) was injected intravenously into the tail vein of mice. At this point, tumor size reached to about 3 mm in diameter according to the preliminary experiment (data not shown). Two, 12 or 24 hr after NK012 or CPT-11 injection, mice were also administered with fluorescein *Lycopersicon esculentum* lectin (100 μl/mouse) (Vector Laboratories, Burlingame, CA) to visualize tumor blood vessels. Tumors were then excised and embedded in optimal cutting temperature compound and frozen at −80°C until use. Tissue sections (6 μm thick) were prepared using Tissue-Tek Cryo3 (Sakura Finetek USA, Inc., Torrance, CA), and frozen sections were examined under a fluorescence microscope, BIOREVO BZ9000 (Keyence, Osaka, Japan), at an excitation wavelength of 377 nm and an emission wavelength 447 nm to evaluate the distribution of CPT-11 and NK012 within the tumor tissues. Because formulations containing SN-38 bound *via* ester bonds possess a particular fluorescence, both CPT-11 and NK012 were detected under the same fluorescence conditions. Image data were recorded using BZ-II Analyzer 1.10 software (Keyence, Osaka, Japan).

Pharmacokinetics study of NK012 and CPT-11

Female BALB/c nude mice bearing U87MG/Luc tumor ($n = 3$) were used for the analysis of the biodistribution of NK012 and CPT-11. Twenty days after the intracranial injection of U87MG/Luc cells, NK012 (30 mg/kg) or CPT-11 (66.7 mg/kg) was intravenously administered to the mice. Under anesthesia, blood, normal brain tissues and tumor tissues were obtained 2, 12, 24 and 72 hr after NK012 or CPT-11 administration. Blood samples were collected in microtubes and immediately centrifuged at 1,600*g* for 15 min at 4°C. All samples were stored at −80°C until use.

The normal brain and tumor samples were rinsed with physiologic 0.9% NaCl solution, mixed with 0.1 M glycine-HCl buffer (pH 3.0)/methanol at 5 w/w%, and then homogenized. To analyze the concentration of free SN-38 and CPT-11, 100 μl of the tumor homogenates was mixed with 20 μl of 1 mM phosphoric acid/methanol (1:1), 40 μl of ultrapure water and 60 μl of camptothecin solution (10 ng/ml for SN-38 and 15 ng/ml for CPT-11) as an internal standard. To quantify free SN-38 and CPT-11 in plasma, 25 μl of plasma was mixed with 25 μl of 0.1 M HCl, and then added with 20 μl of 1 mM phosphoric acid/methanol (1:1) and 100 μl of CPT solution (10 ng/ml both for SN-38 and CPT-11). The samples were vortexed vigorously for 10 sec, and then filtered through Ultrafree-MC centrifugal filter devices with a cut-off molecular diameter of 0.45 μm (Millipore Co., Bedford, MA). Reversed-phase HPLC was performed at 35°C on a Mightysil RP-18 GP column 150 × 4.6 mm^2 (Kanto Chemical Co., Inc., Tokyo, Japan). Fifty microliters of a sample was injected into an Alliance Waters 2795 HPLC system (Waters, Milford, MA) equipped with a Waters 2475 multi λ fluorescence detector. Fluorescence originating from SN-38 was detected at 540 nm with an excitation wavelength of 365 nm and that originating from CPT-11 was detected at 430 nm with an excitation wavelength of 365 nm. The mobile phase was a mixture of 100 nmol/l ammonium acetate (pH 4.2) and methanol (11:9 (v/v)). The flow rate was 1.0 ml/min. The content of SN-38 was calculated by measuring the relevant peak area and calibrating against the corresponding peak area derived from the CPT internal standard. Peak data were recorded using a chromatography management system (MassLynx v4.0, Waters).

For polymer-bound SN-38 detection, SN-38 was released from the conjugate. Briefly, 20 μl of plasma and 100 μl of tissue

TABLE I – IC_{50} VALUES OF SN-38, NK012, CPT-11, ACNU, CDDP AND VP-16 IN VARIOUS HUMAN GLIOBLASTOMA CELL LINES

Cell line	IC_{50}(μmol/l)					
	SN38	NK012	CPT-11	ACNU	CDDP	Etoposide
LN18	0.052 ± 0.0034	0.069 ± 0.0242	13.0 ± 0.88	729 ± 30	3.57 ± 0.08	3.84 ± 0.14
LN229	0.28 ± 0.1094	0.36 ± 0.0489	12.2 ± 1.23	144 ± 23	21.4 ± 0.62	0.945 ± 0.025
U87MG	0.18 ± 0.0216	0.093 ± 0.0038	18.1 ± 3.06	865 ± 86	9.06 ± 0.57	20.8 ± 5.23
U118MG	0.0089 ± 0.0003	0.022 ± 0.0017	4.85 ± 0.14	282 ± 22	3.35 ± 0.35	4.05 ± 0.18
U251MG	0.0076 ± 0.0001	0.0087 ± 0.0002	3.86 ± 0.04	51.6 ± 3.7	4.55 ± 0.03	2.42 ± 0.13

Each cell line was treated in triplicate for 72 hr.
WST–8 assay was used for obtaining IC_{50} value.

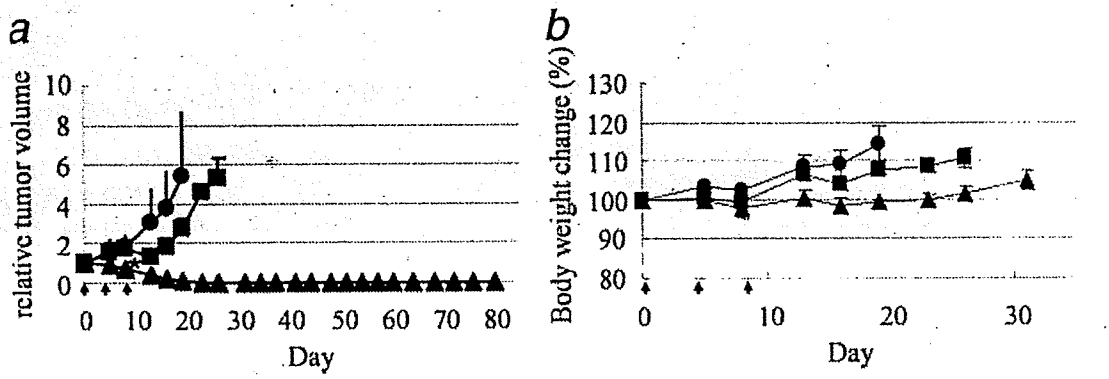

FIGURE 1 – Effects of NK012 and CPT-11 on U87MG/Luc tumor xenograft. (*a*) Tumor volume in mice treated with CPT-11 or NK012. U87MG/Luc tumor was subcutaneously inoculated into the flank of mice, as described in the Materials and methods section. NaCl (0.9%) solution (●), CPT-11 at 66.7 mg/kg (■) and NK012 at 30 mg/kg (▲) were intravenously administered on days 0, 4 and 8 (arrows). Points, mean; bars, SD. *$p < 0.05$. (*b*) Treatment-related body weight loss occurred in mice treated with CPT-11 and NK012. Points, mean; bars, SD.

samples were diluted with 20 μl of methanol (50%, v/v) and 20 μl of NaOH (0.3 mol/l for plasma and 0.7 mol/l for tissue). The samples were incubated for 15 min at 25°C. After incubation, 20 μl of HCl (0.3 mol/l for plasma and 0.7 mol/l for tissue) and 60 μl of CPT solution (10 ng/ml for SN-38 and 15 ng/ml for CPT-11) were added to the samples, and then the hydrolysate was filtered through a MultiScreen Solvinert. Fifty microliters of the filtrate was applied to the same HPLC system as described earlier.

In vivo *growth inhibition assay*

Experiment 1. Six-week-old mice were subcutaneously inoculated with 1×10^7 U87MG/Luc cells in the flank region. When tumor volume reached ~605 mm^3, mice were randomly divided into test groups consisting of 3 mice per group (day 0). Drug was intravenously administered on days 0, 4 and 8 into the tail vein. NK012 was administered at its MTD of 30 mg/kg/day. The reference drug CPT-11 was given at its MTD of 66.7 mg/kg/day in the optimal schedule reported.[17,21] The length (*i*) and width (*ii*) of tumor masses were measured twice a week, and tumor volume (TV) was calculated as follows: $TV = (a \times b^2)/2$. Relative tumor volumes (RTVs) at day *n* were calculated according to the following formula: $RTV = TV_n / TV_0$, where TV_n is the tumor volume at day *n*, and TV_0 is the tumor volume at day 0.

Experiment 2. To assess the antitumor effect of NK012 and CPT-11, *in vivo* bioluminescence imaging studies were performed using the Photon Imager animal imaging system (Biospace, Paris, France). For imaging, mice with intracranial U87MG/Luc tumor were simultaneously anesthetized with isoflurane and d-luciferine potassium salt (Synchem, Germany), and normal 0.9% NaCl solution was intraperitoneally administrated at a dose of 125 mg/kg body weight, and images were obtained 5 min after the injection. For bioluminescence image analysis, regions of interest encompassing the intracranial area of a signal were defined using Photo Vision software (Biospace, Paris, France), and total numbers of photons per minute (cpm) were recorded. The pseudo-color luminescent image from violet (least intense) to red (most intense) represented the spatial distribution of detected photon counts emerging from active luciferase within the animal. Twenty days after U87MG inoculation, treatment was started (day 0). Normal 0.9% NaCl solution ($n = 4$), NK012 (30 mg/kg, $n = 4$), or CPT-11 (66.7 mg/kg, $n = 4$) was intravenously administered to mice on days 0, 4 and 8. *In vivo* bioluminescence imaging studies were performed on days 0, 14, 21 and 28 from the day of treatment initiation. To determine the effect of treatment on the time to change of intensity, Student's *t* test was carried out using the StatView 5.0 software package. $p < 0.05$ was regarded as significant.

Experiment 3. Mice with intracranial U87MG/Luc tumor was randomly divided into 3 groups consisting of 6 mice per group. NK012 (30 mg/kg/day) and CPT-11 (66.7 mg/kg/day) were intravenously given on days 0 (20 days after tumor inoculation), 4 and 8. After treatment, mice were maintained until each animal showed signs of morbidity (*i.e.*, 10% weight loss and neurological deficit), at which point they were sacrificed. Kaplan-Meier analysis was performed to determine the effect of drugs on time to morbidity, and statistical differences were ranked according to the Mantel-Cox log-rank test using StatView 5.0.

Statistical analysis

Data were expressed as mean ± SD. Significance of differences was calculated using the unpaired *t* test with repeated measures of StatView 5.0. $p < 0.05$ was regarded as significant.

Results

Cellular sensitivity of glioblastoma cells to SN-38, NK012 and CPT-11

The IC_{50} values of NK012 for the cell lines ranged from 0.0087 μmol/l (U251MG cells) to 0.36 μmol/l (LN229 cells). The growth inhibitory effects of NK012 were 34- to 444-fold more potent than those of CPT-11, 400- to 12818-fold more potent than those of ACNU, 52-to 523-fold more potent than those of CDDP, and 3- to 278-fold

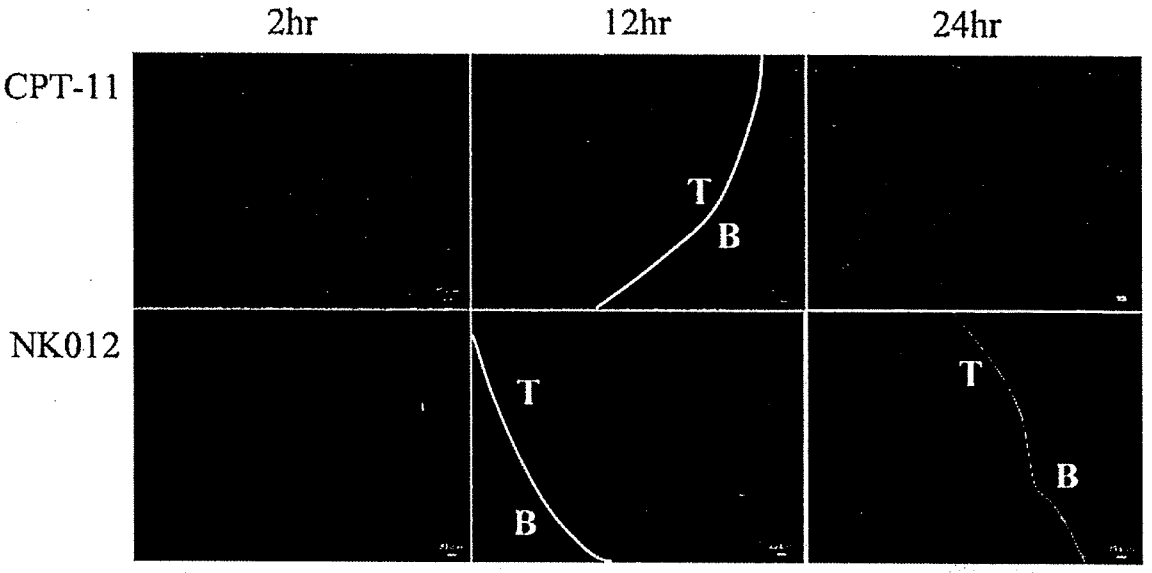

FIGURE 2 – Distribution of NK012 or CPT-11 in U87MG/Luc glioma xenografts. Mice bearing U87MG/Luc tumor were injected with NK012 (30 mg/kg/day) or CPT-11 (66.7 mg/kg/day). Tumor tissues were excised 2, 12 and 24 hr after the intravenous injection of NK012 or CPT-11. Each mouse was administered fluorescein-labeled *Lycopersicon esculentum* lectin 5 min before sacrifice to detect tumor blood vessels. Frozen sections were examined under a fluorescence microscope at an excitation wavelength of 377 nm and an emission wavelength of 477 nm. The same fluorescence conditions can be applied for visualizing NK012 and CPT-11 fluorescence. Free SN-38 could not be detected under these fluorescence conditions. The white lines indicate the border between the tumor and the brain tissue. T, U87MG/Luc tumor; B, normal brain tissue. (Scale bars: 20 μm).

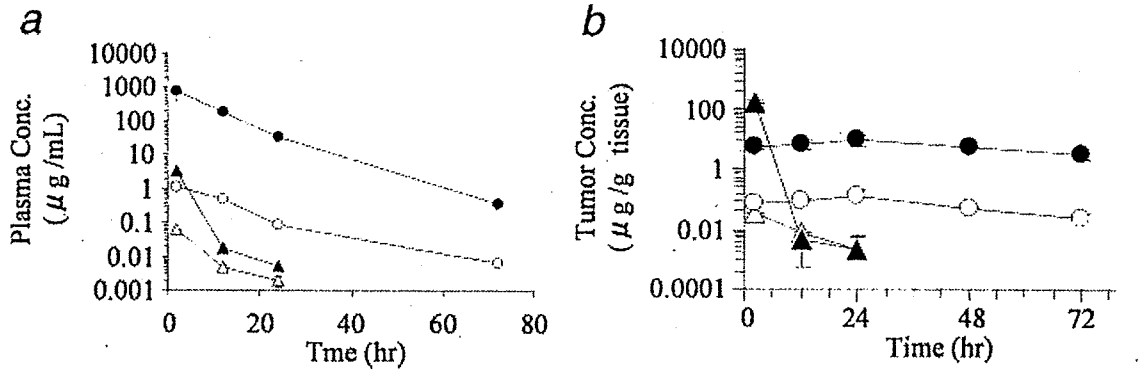

FIGURE 3 – Plasma, brain tissue and orthotopic tumor concentrations of respective analytes after intravenous administration of NK012 (30 mg/kg/day) and CPT-11 (66.7 mg/kg/day) to U87MG/Luc-bearing nude mice. (*a*) plasma; (*b*) tumor. ●, polymer-bound SN-38; ○, free SN-38 (polymer-unbound SN-38); ▲, CPT-11; △, free SN-38 converted from CPT-11.

more potent than those of etoposide. On the other hand, the IC_{50} values of NK012 were almost similar to those of SN-38 (Table. I).

Antitumor activity of NK012 and CPT-11 on subcutaneous U87MG/Luc xenografts

Potent antitumor activity was observed in mice treated with NK012 at 30 mg/kg *in vivo* (Fig. 1*a*). In mice treated with NK012, tumor volume started to decrease on day 5, and the tumor completely disappeared by day 23, with no relapse observed until 80 days after treatment. Although CPT-11 at 66.7 mg/kg/day exerted antitumor activity compared with the control group, tumor volume continued to increase consistently. Comparison of the relative tumor volume at day 8 revealed significant differences between the NK012-treated and CPT-11-treated groups ($p = 0.0095$). Although treatment-related body weight loss was observed in mice treated with each drug, body weight recovery was observed by day 19 (Fig. 1*b*). These results clearly show the significant *in vivo* activity of NK012 against the U87MG/Luc tumor xeonograft.

Studies on distribution of NK012 and CPT-11 in orthotopic U87MG/Luc tumor tissues

Both NK012 and CPT-11 formulations accumulated in the tumor tissue but not in the normal brain tissue (Fig. 2). However, the drug distribution pattern was clearly different between NK012 and CPT-11. In sections of the U87MG/Luc tumor treated with CPT-11, maximum drug accumulation was observed within 2 hr of CPT-11 injection. Twelve hours after the injection, fluorescence originating from CPT-11 had almost disappeared. Subsequently, no accumulation of CPT-11 was observed within the tumor tissues. However, in sections of the U87MG/Luc tumor treated with NK012, fluorescence from NK012 started appearing around tumor blood vessels 2 hr after intravenous injection and lasted until 24

TABLE II – TUMOR AND PLASMA CONCENTRATION OF SN38 AFTER AN I.V. ADMINISTRATION OF NK012 (30 MG/KG) AND CPT-11 (66.7MG/KG) TO NUDE MICE BEARING U87MG/LUC BRAIN TUMOR

Formulation tested	Analyte		Time after administration (hr)			
			2	12	24	72
NK012	Free SN-38	Plasma (ng/ml)	1113	511	90.0	6.88
		Tumor (ng/g)	67.7	84.1	137	24.6
CPT-11	Free SN-38 5	Plasma (ng/ml)	62.0	4.74	1.97	ND
		Tumor (ng/g)	31.8	7.41	2.14	ND

Data were expressed as means of three mice.
Free SN-38; SN-38 released from NK012 or converted from CPT-11.
ND, not detectable.

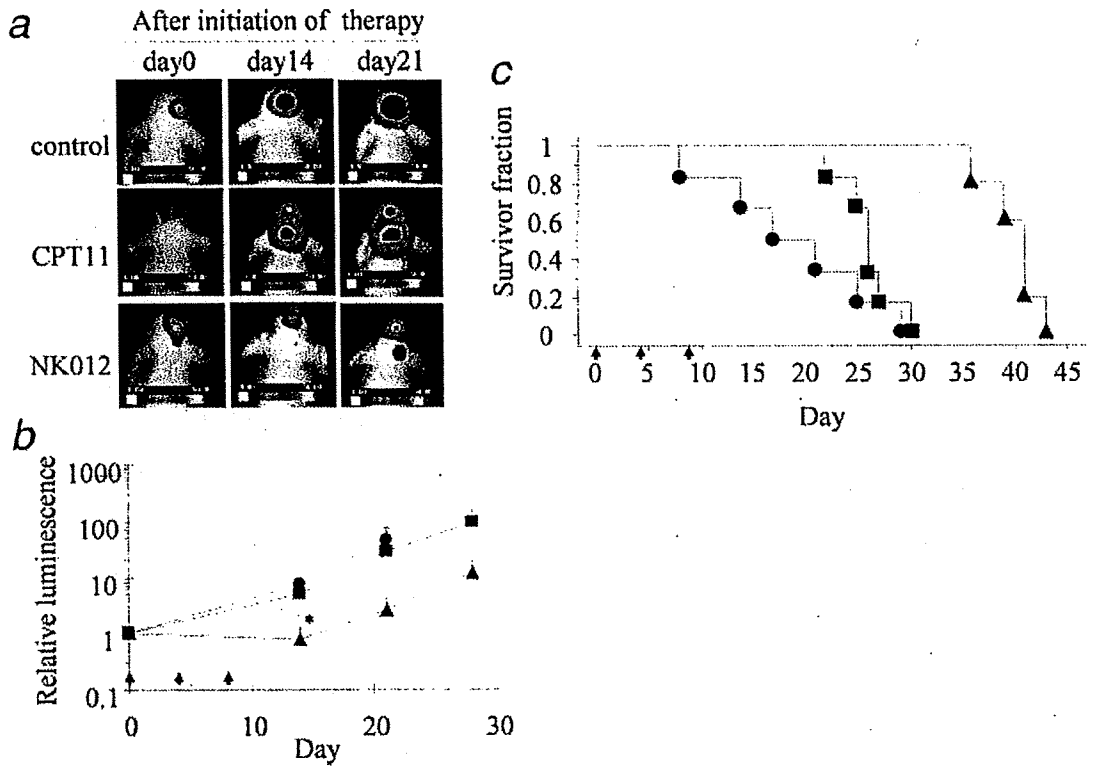

FIGURE 4 – Antitumor effect of NK012 or CPT-11 on orthotopic xenograft and survival. Mice receiving intracranial injections of U87MG/Luc were assigned into groups 20 days after tumor inoculation. Mice were intravenously administered with 0.9% NaCl solution (●), NK012 (30 mg/kg/day, ▲) or CPT-11 (66.7 mg/kg/day, ■) on days 0 (20 days after tumor inoculation), 4 and 8 (arrows). (*a*) Representative luminescence intensity images obtained in individual control and treatment-group mice on the days indicated. (*b*) Antitumor effect of NK012 or CPT-11 on days 14, 21 and 28. Each group consisted of 4 mice. Points, mean; bars, SD. $*p < 0.05$. (*c*) Treatment effects of NK012 on survival. Survival was assessed by Kaplan-Meier analysis. Each group consisted of 6 mice. Experiments were repeated twice with similar results.

hr. After 12 hr, the fluorescent area began to increase and the maximum fluorescence area was observed 24 hr after the injection.

Pharmacokinetics analysis of NK012 and CPT-11 in mice bearing orthotopic U87MG/Luc xenografts

Microscopic observations were confirmed quantitatively by measuring the amount of SN-38 extracted from each solid tumor by reversed-phase HPLC. After CPT-11 injection, the concentrations of CPT-11 and free SN-38 in plasma decreased rapidly with time in a log-linear fashion. On the other hand, the plasma concentration of NK012 (polymer-bound SN-38) showed slower clearance than that of CPT-11. Free SN-38 released from NK012 also showed slow clearance than that of SN-38 converted from CPT-11 (Fig. 3*a*). Meanwhile, there was a significant difference in drug accumulation in the tumor between CPT-11 and NK012, that is, the accumulation of NK012 in the U87MG/Luc tumor was significantly higher than that of CPT-11 (Fig. 3*b*) and that the concentration of free SN-38 originating from NK012 was maintained at 24.6 ng/g even 72 hr after injection (Table II). On the other hand, only slight conversion from CPT-11 to SN-38 was observed from 2 to 24 hr in the U87MG/Luc tumor, and no SN-38 was detected thereafter (Fig. 3*b*). This result suggests that the BTB of the tumor was partially destroyed in the tumor vasculature and both drugs extravasated from the tumor blood vessels. In addition, these results indicate that NK012 can remain in the tumor tissue for a longer period and continue to release free SN-38.

Antitumor activity of NK012 and CPT-11 against orthotopic U87MG/Luc glioma xenografts

Antitumor activity was observed in mice treated with NK012 at 30 mg/kg/day and CPT-11 at 66.7 mg/kg/day *in vivo* (Fig. 4*a*). ANOVA analysis revealed a significant difference between the control group and the NK012-treated group ($p = 0.02$). However there was no significant difference between the control group and

the CPT-11-treated group ($p = 0.23$) and between NK012 and CPT-11 ($p = 0.21$) (Fig. 4*b*). Comparison of the relative tumor volume at day 14 revealed significant differences between NK012 (30 mg/kg/day) and CPT-11 (66.7 mg/kg/day) ($p = 0.049$). Kaplan-Meier analysis showed that a significant improvement in survival rate was observed in the NK012 treatment group compared with the control ($p = 0.001$) and CPT-11 treatment groups ($p = 0.0014$) (Fig. 4*c*).

Discussion

The diameter of a micelle carrier is approximately in the range of 10–100 nm, which is smaller than that of a liposome. Although this size is small, it is still sufficiently large to prevent renal secretion of the carrier. The micelle systems can evade nonspecific capture by the reticuloendothelial system in various organs because the outer shell of the micelle is covered with polyethyleneglycol. Therefore, drug-incorporating micelles can be expected to have a long plasma half-life, which permits a large amount of the micelles to reach tumor tissues, extravasate from tumor capillaries, and then be retained in tumor tissues for a long time by utilizing the enhanced permeability and retention (EPR) effect.[22]

Several factors are reportedly involved in vascular permeability in the body. Among them, bradykinin is the most potent vascular permeability factor. We succeeded in purifying 2 types of kinin from the ascitic fluid of a patient with gastric cancer.[23] We also clarified that this kinin generation system was triggered by the activated Hageman factor, an intrinsic coagulation factor XII.[24] Meanwhile, Dvorak et al. discovered that the vascular permeability factor (VPF) is involved in tumor vascular permeability.[25] Later, it was found that VPF was identical to VEGF.[26] Recently, an extrinsic coagulation factor, namely, a tissue factor, has been shown to activate VEGF production.[27,28] Thus, both intrinsic and extrinsic coagulation factors may be involved in tumor vascular permeability. Furthermore, there have been several reports to date indicating the increasing expression of a tissue factor in human glioma.[29,30] Also, it is well known that glioma is a typical hypervascular tumor with an irregular vascular architecture and a high expression level of VEGF.[31] Therefore, it may be speculated that nanoparticles extravasate from tumor capillaries and accumulate more preferentially in brain glioma.

NK012, an SN-38-incorporating polymeric micelle, is a novel type of micellar formulation with long-time accumulation in tumors, and shows prolonged sustained release of SN-38 within the tumor.[17,20] We have thus far reported that NK012 shows significantly higher antitumor activity against various human tumor xenografts including small cell lung cancer,[17] colorectal cancer,[19] renal cancer,[18] and pancreatic cancer[20] compared with CPT-11. In addition, we have recently seen an increasing number of reports of clinical trials indicating the effectiveness of CPT-11 against brain glioma in combination with anti-VEGF antibody[11,12,32,33]

Under these circumstances, it may be reasonable to conduct an investigation into the advantages of administering NK012 over CPT-11 for treatment against human glioma tumor xenografts. In the present study, we showed that NK012 exerted a significant antitumor activity in U87MG/Luc subcutaneous xenografts (Fig. 1). In the tumor intravenously administered with NK012 (30 mg/kg), NK012 accumulated within and around tumor blood vessels in the orthotopic xenografts 2 hr after the injection. Thereafter, NK012 started to spread from the blood vessel within the tumor tissue of the xenografts. Fluorescence originating from NK012 then increased up to the maximum in the entire tumor by 24 hr after NK012 injection. On the other hand, fluorescence originating from CPT-11 increased up to the maximum 2 hr after its injection, indicating that the maximum distribution of CPT-11 was achieved within 2 hr of injection. Twelve hours after intravenous injection, fluorescence from CPT-11 had almost disappeared, and subsequently, no accumulation of CPT-11 was observed within the tumor tissues. The therapeutic effect of NK012 was superior to that of CPT-11 in terms of antitumor effect and survival. Because the antitumor activity of SN-38 is time-dependent, the superiority of NK012 over CPT-11 may be due to the enhanced accumulation of NK012 and the prolonged sustained release of SN-38 from NK012 within the tumor tissues. Nevertheless, free SN-38 was not detected in the normal brain tissues at any measurement time after intravenous injection of NK012 or CPT-11 (data not shown). It is thus speculated that both NK012 and CPT-11 are unable to cross the BBB in the normal brain, but can pass through tumor vessels effectively. In clinical brain glioma, however, when the tumor recurs, it would most likely recur in adjacent regions of the brain with an intact blood brain barrier. Namely, at the border between the brain tumor and normal brain tissue, malignant glioma cells and normal brain tissues intermix in the gradient and angiogenesis occurs at sites where there are large accumulation of tumor cells under local hypoxia.[34] In addition, there is no clear evidence if tumor vessels of orthotopic brain tumor xenografts are identical to those of real human brain tumors in terms of their structure and function. Therefore, it may be better to consider to conduct an investigation of the advantages of administering some anti-angiogenic inhibitors in combination with NK012 against highly invasive tumor models established by several methods such as direct implantation of patient surgical specimens into the brains of nude mice,[35] transplantation of patient surgical material s.c. in nude mice followed by dissociation and orthotopic reinjection of these xenotransplants,[36] engraftment of glioblastoma-derived spheroids after short- term culture into rat brain,[37] and engraftment of glioblastomastem cell-enriched cultures into mouse brain.[38,39]

The dose-limiting toxicities of CPT-11 appeared to be neutropenia and diarrhea. However, in our previous data, there was no significant difference in the level of SN-38 in the small intestine between NK012-treated and CPT-11-treated mice.[17] It was also reported that NK012 showed significant antitumor effect with diminishing incidence of diarrhea compared with CPT-11.[40] In 2 individual phase 1 trials in Japan and the US, no serious diarrhea has been reported.[41,42] In addition, one confirmed partial response (PR) was obtained in a patient with metastatic esophageal cancer in a Japanese trial,[41] and 3 PRs in a patient with breast cancer and 1 PR in a patient with small cell lung cancer in a US phase 1 trial.[42]

In conclusion, we demonstrated not only the enhanced accumulation, distribution, and retention of NK012 within glioma xenografts but also the superiority of the antitumor activity of NK012 compared with CPT-11. Taking the present data together with very recent clinical data from phase 1 trials, a phase 2 trial in patients with recurrent glioma may be warranted.

Acknowledgements

The authors thank Ms. N. Mie, Ms. H. Miyatake and Ms. M. Ohtsu for their technical assistance and Ms. K. Shiina for her secretarial assistance.

References

1. DeAngelis LM. Brain tumors. N Engl J Med 2001;344:114–23.
2. Kleihues P, Louis DN, Scheithauer BW, Rorke LB, Reifenberger G, Burger PC, Cavenee WK. The WHO classification of tumors of the nervous system. J Neuropathol Exp Neurol 2002;61:215–25 discussion 26–9.
3. Stupp R, Mason WP, van den Bent MJ, Weller M, Fisher B, Taphoorn MJ, Belanger K, Brandes AA, Marosi C, Bogdahn U, Curschmann J, Janzer RC, et al. Radiotherapy plus concomitant and adjuvant temozolomide for glioblastoma. N Engl J Med 2005;352:987–96.
4. Wong ET, Hess KR, Gleason MJ, Jaeckle KA, Kyritsis AP, Prados MD, Levin VA, Yung WK. Outcomes and prognostic factors in recurrent glioma patients enrolled onto phase II clinical trials. J Clin Oncol 1999;17:2572–8.